Title: Downregulation of muscle cell *Insr* and insulin receptor signaling by hyperinsulinemia *in vitro* and *in vivo*

Authors: Haoning Howard Cen, José Diego Botezelli, Su Wang, Niloufar Noursadeghi, James D. Johnson*

Affiliation: Department of Cellular and Physiological Sciences, Life Science Institute, University of British Columbia, Vancouver, BC. Canada.

Running title: Hyperinsulinemia-induced insulin resistance

Keywords: insulin, insulin receptor, insulin resistance, skeletal muscle, FOXO

***Address correspondence to:** James D. Johnson, Ph.D., Professor. Diabetes Research Group, Dept. of Cellular and Physiological Sciences & Dept. of Surgery, University of British Columbia, 5358 Life Sciences Building, 2350 Health Sciences Mall, Vancouver, BC, Canada, V6T 1Z3
E-mail: James.D.Johnson@ubc.ca; Fax: (604) 822-2316
Twitter: @JimJohnsonSci

Disclosure Statement: The authors have no relevant conflicts of interest to disclose.

Abstract

Hyperinsulinemia is often viewed as compensatory to insulin resistance, but studies have shown that high levels of insulin may also contribute to insulin resistance. The precise mechanisms by which hyperinsulinemia contributes to insulin resistance remain poorly defined. To understand the direct effects of prolonged exposure to excess insulin in muscle cells, we incubated differentiated C2C12 mouse myotubes with elevated insulin for 16 hours, followed by 6 hours serum starvation, before examining key insulin signaling nodes. Using this model, we found that prolonged high insulin treatment significantly increased the phosphorylation of insulin receptor (INSR) and AKT, but not ERK. After serum starvation, acute AKT and ERK signaling stimulated by 0.2 - 20 nM insulin was attenuated. INSR protein levels were significantly downregulated by hyperinsulinemia in an insulin-dose-dependent manner. Surface INSR was reduced proportionally to total INSR levels. Mechanistically, we found that hyperinsulinemia strongly downregulated *Insr* mRNA which was correlated with increased threonine 24 phosphorylation of FOXO1. Interestingly, 6h serum starvation reversed the effects of high insulin on basal phosphorylation of INSR, AKT and FOXO1, and *Insr* transcription. Using RNA sequencing, bioinformatic analysis, and follow-up RNAi studies, we identified SIN3A as a negative regulator of *Insr* mRNA levels and JUND, MAX and MXI as positive regulators of *Irs2* mRNA. We validated our *in vitro* results by determining that INSR levels in mouse skeletal muscle were negatively correlated with circulating insulin *in vivo*. Together, our findings shed new light on the mechanisms underlying hyperinsulinemia-induced insulin resistance in muscle cells, which are likely to be relevant in the pathogenesis of type 2 diabetes.

48 **Introduction**

49 Hyperinsulinemia and insulin resistance are cardinal features of type 2 diabetes (T2D) and
50 highly associated with each other. It has been a widely held view that insulin resistance is the
51 primary cause of type 2 diabetes and that hyperinsulinemia is a compensatory response (1,2).
52 However, a growing body of evidence suggests the opposite may be true in many cases (3-5).
53 Hyperinsulinemia can be observed prior to insulin resistance in obesity and T2D (6-8) and
54 hyperinsulinemia is the strongest predictor of T2D in long-term studies (9,10). We recently
55 showed that hyperinsulinemia contributes causally to age-dependent insulin resistance in the
56 absence of hyperglycemia (11). Reducing hyperinsulinemia in partial insulin gene knockout mice
57 prevents and reverses diet-induced obesity in adult mice (11-13). Rodents (14,15), healthy
58 humans (16,17), and people with type 1 diabetes (18) subjected to prolonged insulin
59 administration also have reduced insulin responsiveness independent of hyperglycemia. This
60 strongly suggests that hyperinsulinemia is a self-perpetuating cause of insulin resistance.

61 The mechanisms by which hyperinsulinemia contributes to insulin resistance remain poorly
62 understood. The insulin receptor (INSR) is a critical component as the starting point of insulin
63 action. It has been reported that obese or diabetic rodent models with hyperinsulinemia and
64 insulin resistance have reduced insulin binding to the liver (19,20), fat (21) and pancreatic acinar
65 cells (22). The reduction in insulin binding may be due to INSR downregulation rather than
66 immediate changes in binding affinity, since chronic (2-16 hours), but not acute, high insulin
67 exposure directly reduced insulin binding and INSR protein levels in adipocytes (23) and
68 lymphocytes (24) *in vitro*. However, the molecular mechanisms of INSR down-regulation and
69 post-receptor insulin resistance remain poorly characterized in muscle cells.

70 In the present study, we employed an *in vitro* model of insulin resistance using a muscle cell
71 line and confirmed our observations *in vivo* using mice with variable hyperinsulinemia. We found
72 that hyperinsulinemia induced insulin resistance featuring blunted acute insulin signaling and
73 transcriptional INSR downregulation associated with reduced FOXO1 activity. Transcriptome
74 wide consequences of hyperinsulinemia were also characterized, revealing *Sin3a* as a novel
75 transcription factor suppressing *Insr* expression. Our data illuminate new mechanisms by which
76 hyperinsulinemia contributes to insulin resistance in muscle cells.
77

78 **Results**

79 ***Hyperinsulinemia induces insulin resistance in muscle cells in vitro***

80 Circulating insulin in humans oscillates in a range between 0.03 nM and 1.9 nM, and fasting
81 insulin less than 0.17 nM is considered normal (25). To establish a muscle cell model of
82 hyperinsulinemia-induced insulin resistance, we incubated differentiated mouse C2C12 myotubes
83 for 16 hours in a physiologically high insulin dose of 2 nM or supraphysiologically high dose of
84 200 nM (Fig. 1A). Hyperinsulinemia was confirmed after treatment with high insulin (Fig. 1A').
85 After 6-hour serum starvation, insulin signaling was characterized by measuring the
86 phosphorylation of AKT and ERK proteins, which represent two major insulin signaling nodes (26).
87 Since alterations in the basal state of the insulin signal transduction network have also been
88 reported in hyperinsulinemic humans and animals (27), we also measured the effects of
89 hyperinsulinemia on AKT and ERK phosphorylation before and after serum starvation. These
90 experiments showed that total AKT protein levels were significantly downregulated by prolonged
91 200 nM, but not 2 nM, insulin treatment, while ERK abundance was not significantly changed (Fig.
92 1B-D). After prolonged 200 nM insulin exposure and before serum starvation, AKT

93 phosphorylation at threonine (T) 308 and serine (S) 473 was significantly elevated, but ERK
94 phosphorylation was unaffected (Fig. 1E,F). Of note, phosphorylation of ERK1/2 was increased
95 by serum starvation alone, as previously reported in other cell types (Fig. 1F)(28). Acute AKT and
96 ERK signaling in the context of 2 nM acute insulin was significantly reduced by hyperinsulinemia
97 treatment in an insulin dose-dependent manner (Fig. 1E,F). We also characterized the insulin
98 dose- and time-dependent signaling in our *in vitro* hyperinsulinemia model (200 nM insulin).
99 Phosphorylation of AKT and ERK1/2 were significantly reduced under 0.2, 2, or 20 nM insulin
100 stimulations (Fig. 2A,B). Together, these results establish a robust muscle cell insulin resistance
101 model induced by hyperinsulinemia and characterized its effects on basal and acute insulin
102 signaling.
103

104 ***Hyperinsulinemia reduces INSR protein abundance but not its phosphorylation or***
105 ***internalization***

106 To better understand the effects of hyperinsulinemia on the earliest stages of insulin
107 signalling, we examined on INSR abundance, phosphorylation, and internalization. Remarkably,
108 we found the total INSR protein abundance was robustly decreased in both hyperinsulinemia
109 groups in an insulin dose-dependent manner (Fig. 3A, B). Serum starvation slightly recovered the
110 INSR downregulation in 200 nM insulin group (Fig. 3B). These results clearly demonstrated that
111 hyperinsulinemia can modulate INSR abundance in this cell system.

112 We also examined INSR tyrosine 1150/1151 autophosphorylation, which is an early step of
113 insulin signaling that recruits IRS and SHC, leading to PI3K-AKT or RAS-ERK activation (26).
114 Before starvation, both hyperinsulinemia groups had increased INSR phosphorylation, suggesting
115 that there was continuous insulin signaling during the high insulin treatments (Fig. 3C). Serum

116 starvation completely reversed INSR hyperphosphorylation (Fig. 3C). While INSR
117 phosphorylation was not significantly different after 10 min of acute insulin stimulation (Fig. 3C),
118 analysis of dose- and time-dependent insulin signaling revealed a tendency for increased
119 phosphorylated-to-total INSR ratio in insulin-stimulated cells exposed overnight to 200 nM insulin
120 (Fig. 3D). The increased INSR phosphorylation per receptor was offset by the reduced INSR
121 number, leading to a decreased phospho-INSR-to-tubulin ratio (i.e. the overall INSR
122 phosphorylation events per cell) (Fig. 3D). These data indicate that the were not defects in INSR
123 phosphorylation upon acute insulin stimulation in our system.

124 Impaired INSR endocytosis has been implicated in insulin resistance (29,30). Therefore,
125 basal surface INSR, as well as dose- and time-dependent INSR internalization were examined in
126 our hyperinsulinemia model using a surface biotinylation assay (Fig. 4A). Serum starvation slightly
127 decreased surface-to-total INSR ratio, while hyperinsulinemia had no significant effects (Fig. 4B).
128 Upon acute insulin stimulation, the internalized INSR to total INSR ratio did not have evident
129 differences except for a small increase when stimulated by 2 nM insulin (Fig. 4C). Therefore,
130 hyperinsulinemia-induced insulin resistance may be mediated by a reduction in total INSR that
131 results in a proportional reduction in INSR protein at the cell surface. The fraction of INSR
132 internalized during acute insulin signaling was not drastically affected by hyperinsulinemia under
133 these conditions. Collectively, our experiments suggest that hyperinsulinemia-induced insulin
134 resistance in muscle cells is mediated in large part by a reduction in total INSR, and not by
135 affecting its activity or internalization.

136

137 ***Circulating insulin negatively correlates with INSR level in vivo***

138 To validate our *in vitro* studies, we examined the relationship between *in vivo* insulin

139 concentration and muscle INSR levels in mice. As in our previous studies (12), insulin gene
140 dosage was manipulated (*Ins1*$^{+/+}$;*Ins2*$^{-/-}$ and *Ins1*$^{+/-}$;*Ins2*$^{-/-}$) to generate variance in circulating
141 insulin. The mice were fed with high fat diet (HFD) known to induced pronounced hyperinsulinemia
142 (12,31) or low fat diet (LFD). These experiments showed that INSR protein abundance negatively
143 correlated with both fasting insulin and fasting glucose in the HFD group (Fig. 5A-B). However,
144 the LFD group only had a negative correlation between INSR level and insulin, with no correlation
145 between INSR and glucose (Fig. 5C-D). These data support the concept that insulin, independent
146 from glucose, can negatively regulate INSR levels in skeletal muscle. This is consistent with our
147 *in vitro* hyperinsulinemia model and our previous *in vivo* data demonstrating improved insulin
148 sensitivity over time in mice with genetically reduced insulin production (11). These data also
149 suggest an interaction between insulin, glucose and INSR that is dependent on the conditions of
150 the HFD.
151

152 ***Hyperinsulinemia reduces Insr mRNA alongside FOXO1 inhibition***

153 One possible cause of INSR downregulation would be the reduced expression of the *Insr*
154 gene (22). To test this hypothesis, we measured the mRNA of *Insr* isoforms A and B (*Insr-A* and
155 *Insr-B*) by qPCR. In our hands, *Insr-A* is the predominant isoform in C2C12 myotubes (Fig. 6A).
156 Both *Insr-A* and *Insr-B* mRNA were equally and robustly downregulated after hyperinsulinemia
157 and partially recovered by serum starvation (Fig. 6A), consistent with the change of INSR protein
158 abundance. Interestingly, insulin-like growth factor 1 receptor (*Igfr1*), which has similar structure
159 and signaling as INSR, was also reduced by hyperinsulinemia at the transcriptional level (Fig. 6B).
160 Alteration in *Insr* alternative splicing has been implicated in hyperinsulinemia (32). In our model,
161 the ratio of *Insr-A* and *Insr-B* mRNA was not affected by hyperinsulinemia or serum starvation (Fig.

162 6C). Our evidence suggests that hyperinsulinemia and serum starvation regulate INSR protein
163 abundance by regulating *Insr* mRNA levels.

164 Forkhead box protein O1 (FOXO1) is a known transcriptional regulator of the *Insr* gene and
165 is also a key mediator of insulin signaling (33-35). In *Drosophila* and mouse myoblasts, FOXO1
166 activity is necessary and sufficient to increase *Insr* transcription under serum fasting and reverse
167 this effect in the presence of insulin (34). Therefore, we sought to determine the activity of FOXO1
168 in our hyperinsulinemic model. Indeed, high insulin increased FOXO1 phosphorylation on T24,
169 which is an AKT-associated event known to exclude FOXO1 from the nucleus and decrease its
170 transcriptional activity (36), but did not affect total FOXO1 abundance (Fig. 6D). T24
171 phosphorylation of FOXO1 significantly decreased after starvation (Fig. 6D), consistent with our
172 observed effects on AKT phosphorylation and *Insr* transcription. Our data therefore support the
173 work of other groups indicating a role for FOXO1 in *Insr* gene expression. However, knocking
174 down *Foxo1* mRNA by 40% was insufficient to alter *Insr* mRNA level in C2C12 myoblast (n=5,
175 data no shown), suggesting the possibility of additional redundancy associated with either the
176 remaining 60% of FOXO1 expression or other proteins.

177

178 ***Hyperinsulinemia and serum starvation remodels transcriptome***

179 To further investigate the mechanisms of hyperinsulinemia-induced insulin resistance and
180 to identify new molecular targets, we conducted RNA sequencing (RNAseq) to illustrate the effects
181 of prolonged insulin and serum starvation. We compared the transcriptomes of 5 cultures in each
182 of 4 treatment groups (0 nM or 200 nM insulin, both before and after serum starvation). Principle
183 component analysis (PCA) of RNAseq data showed distinct clustering by hyperinsulinemia or
184 starvation after hyperinsulinemia, but not by starvation itself (Fig. 7A). Many interesting genes

185 previously linked to metabolism and diabetes were differentially expressed between control and
186 hyperinsulinemic groups both before and after serum starvation (Fig. 7B). Several genes that are
187 altered by hyperinsulinemia before starvation changed in the opposite direction after serum
188 starvation, including *Irs2* (Fig. 7B). Through KEGG pathway enrichment analysis, we found that
189 the top pathways upregulated by hyperinsulinemia were related to transcription, translation and
190 DNA repair (Fig. S1A), while the top downregulated pathways included FOXO signaling, RAS,
191 and MAPK signaling (Fig. 7C). Many of these downregulated pathways were upregulated by
192 starvation (200 nM, BS vs AS), but also remained downregulated after starvation (AS, 0 vs 200
193 nM) (Fig. 7C). We focused on the effects of hyperinsulinemia before starvation and the genes
194 altered in the pathways closely related to insulin signaling by protein-protein interaction network,
195 such as insulin signaling, FOXO signaling, PI3K-AKT signaling, and RAS and MAPK signaling
196 pathways (Fig.7D, E, Fig. S1B,C). Altered components of these signaling pathways of interest
197 were also mapped onto KEGG pathways (Fig. S2A-E). Of note, many genes of key insulin
198 signaling proteins were downregulated by hyperinsulinemia, including *Insr*, *Irs1*, *Irs2*, *Akt3*, *Pik3ca*,
199 *Pik3cb*, and *Pik3r3*. Hyperinsulinemia has been previously shown to downregulate insulin
200 signaling proteins such as IRS1 and IRS2 (37,38). Overall, our transcriptomics data revealed
201 strong, reciprocal effects of prolonged hyperinsulinemia and insulin removal on insulin signaling
202 genes.
203

204 ***Novel transcription factors regulate Insr expression and transcriptomic remodeling by***
205 ***insulin***

206 Next, we bioinformatically predicted the upstream transcriptional regulators using a
207 transcriptional factor-gene network built from the differentially expressed genes (Fig. 8A). The top

208 30 transcriptional factors with high degree of connections to altered genes (Fig. 8A), were
209 compared to common transcription factor binding sites of several differentially expressed genes
210 that encode key proteins in insulin signaling (Fig. 8B). The resulting 11 transcription factors were
211 deemed candidates to affect the transcriptional changes in *Insr* and other insulin signaling genes
212 during hyperinsulinemia (Fig. 8B). To investigate the role of these transcription factors on *Insr*
213 expression, we conducted siRNA knockdown for each transcription factor, with knockdown
214 efficiencies varying between 45% and 85% (Fig. 8C). *Sin3a* knockdown (~70%) resulted in a
215 significant increase in *Insr* mRNA, indicating that this transcription factor has a repressive effect
216 (Fig. 8D). In addition, we also assessed the expression of *Irs2*, which had larger fold change than
217 *Insr* upon hyperinsulinemia and starvation. Knockdown of *Jund*, *Max*, and *Mxi1* downregulated
218 *Irs2*, which suggested that these transcription factors are involved in *Irs2* transcription and may
219 contribute to insulin resistance (Fig. 8D). In conclusion, we identified transcription factors for *Insr*
220 and *Irs2* genes among the predicted upstream transcriptional regulators.
221

222 **Discussion**

223 The goal of this study was to explore the mechanisms of hyperinsulinemia-induced insulin
224 resistance in skeletal muscle cells. We demonstrated that prolonged physiological and
225 supraphysiological hyperinsulinemia induced a reduction of AKT and ERK signaling (Fig. 8E).
226 Remarkably, while serum starvation partially reversed the effects of overnight hyperinsulinemia,
227 much of the impaired acute insulin signaling was sustained after 6 hours of insulin withdrawal and
228 serum starvation, suggesting that long-term molecular changes underlie these differences. The
229 effects of prolonged hyperinsulinemia were insulin dose-dependent from the physiological to the
230 supraphysiological range. We demonstrated that the impaired insulin response in our system can

231 be partially accounted for by INSR downregulation at the transcription level via FOXO1
232 phosphorylation, and also used transcriptomic profiling to discover new factors that regulate
233 insulin signalling in our system including SIN3A, JUND, MAX, and MXI1.

234 Our *in vitro* cell culture model provided a robust and controlled system for examining the
235 direct effects of excess insulin, and insulin withdrawal, on multiple components of insulin signaling
236 in muscle cells. Our results are consistent with other *in vitro* cell culture systems designed to
237 examine the effects of hyperinsulinemia. For example, reduced AKT and ERK signaling and INSR
238 abundance were also reported in hyperinsulinemia-treated β-cells (INS1E cell line and rat islets)
239 and enteroendocrine L cells (39,40). Insulin exposure over 3 days blunted IRS1 and AKT
240 phosphorylation in human muscle derived cells (41). Nevertheless, the mechanisms of sustained
241 alterations in AKT and ERK phosphorylation were not fully understood. In our experiments, there
242 were suppressed AKT and ERK phosphorylation at all time points, suggesting that the insulin
243 resistance we observed was impaired responsiveness consistent with signaling deficiencies at
244 both the receptor level and in post-receptor components (42). Indeed, multiple components of
245 insulin signaling were reduced at the transcriptional level revealed by RNAseq, including *Akt3*
246 which is consistant with the reduced AKT protein abundance. We speculate that the proteosome
247 may also be involved because IGF1 treatment can cause proteasome-dependent downregulation
248 of AKT protein (43). Our observations verified the distinct responses to hyperinsulinemia on the
249 bifurcate insulin signaling pathways. Chronic 200 nM insulin treatment preferentially increased
250 basal AKT phosphorylation as a sign of sustained activation, but did not increase the basal ERK
251 phosphorylation, possibly due to desensitization, as reported in neurons (44). Diet- and
252 hyperinsulinemia-induced insulin resistance is generally considered to be related specifically to
253 AKT phosphorylation. Interestingly, chemical inhibition of AKT pathway, but not ERK pathway,

254 has been reported to protect insulin resistance both *in vitro* and *in vivo* (44,45). Further work is
255 required to understand the interplay between INSR expression and both major branches of
256 downstream signaling.

257 A major observation of our work is that hyperinsulinemia directly reduced *Insr* mRNA in
258 cultured cells, consistent with reports from other cell culture systems (22,46). In a previous study,
259 we observed a ~20% increase in *Insr* mRNA from skeletal muscle samples of *Ins1*$^{+/-}$;*Ins2*$^{-/-}$ mice
260 compared to *Ins1*$^{+/+}$;*Ins2*$^{-/-}$ mice, as well as a trend of a ~50% increase in *Foxo1* mRNA (12). Our
261 *in vivo* data in mice are also consistent with the limited data from human studies. For example,
262 T2D patients with higher fasting insulin were found to have lower *Insr* mRNA expression in skeletal
263 muscle biopsies (47). While relative hyperglycemia can increase *Insr* expression in lymphocyte
264 and cancer cell lines (48,49), high glucose inhibits β-cell *Insr* expression through autocrine insulin
265 action and INSR-FOXO1 signaling (48,49). Interestingly, glucose could only induce insulin
266 resistance in the presence of insulin in cultured hepatocytes, adipocytes and skeletal muscle
267 (21,50,51). Therefore, reduced *Insr* expression by hyperinsulinemia may be a key, independent
268 factor of INSR downregulation and insulin resistance.

269 Intermittent fasting, time-restricted feeding, caloric restriction, and/or carbohydrate restriction
270 have been shown to have health benefits in diabetes, including reducing hyperinsulinemia,
271 increasing insulin sensitivity, improving β-cell responsiveness, and lowering the levels of
272 circulating glucose (52-54). Several human trials suggest that fasting regimes can be more
273 effective for reducing insulin and increasing insulin sensitivity than they are for reducing glucose
274 (55,56). By mimicking the low-insulin state, the serum starvation phase of our studies revealed
275 some possible molecular mechanisms of the beneficial effects of fasting on muscle cells, which
276 includes the restoration of protein phosphorylation in insulin signaling pathways and partial

277 recovery of *Insr* transcription and INSR protein. These data hint that some deleterious effects of
278 hyperinsulinemia are reversible but may require a long enough low-insulin period.

279 RNAseq results revealed broad effects of hyperinsulinemia and serum starvation on insulin
280 signaling and FOXO signaling pathways, and highlighted protential upstream transcription factors.
281 Besides FOXO1, other transcription factors such as SP1, HMGA1, C/EBPβ, and NUCKS have
282 been reported to regulate *Insr* expression (57-59), but their role in hyperinsulinemia will require
283 further investigation. We identified at least one novel transcriptional repressor of the *Insr* gene,
284 SIN3A, which was upregulated by hyperinsulinemia. SIN3A interacts with histone deacetylases
285 to inhibit transcription and interacts with other transcription factors that were found in our
286 transcriptomics/bioformatics analyses (60). For example, SIN3A and MYC inhibits each other and
287 form a negative feedback loop (61). MAX dimerizes with either MYC or MXI1 (MAD family protein)
288 in a competing manner to activate or repress target genes (62), and MXI1 recruits SIN3A for gene
289 inhibition (62). Interestingly, the knockdown level we achieved for MYC, MAX, MXI1 did not have
290 significant effects on transcripiton of *Insr*. One possibility is that the roles of these transcrioption
291 factors on *Insr* are indirect and rely on the action of SIN3A, while another possibility is that SIN3A
292 acts through alterative pathways. A recent study identified SIN3A as a FOXO1 corepressor of the
293 glucokinase gene in liver (63). Additional studies will be required to elucidate possible interactions
294 between SIN3A and FOXO1 on the downregulation INSR in our system.

295 The present study has limitations and leaves many questions unanswered. We employed a
296 16-hour insulin incubation instead of a more chronic, multiday hyperinsulinemia treatment. The
297 main reason for this is that insulin promotes the further differentiation of C2C12 myotubes (64),
298 meaning that chronic treatment during differentiation would likely introduce unmanageble
299 variance in the muscle cell model. Our study cannot rule out effects of hyperinsulinemia on INSR

300 protein degradation and overall proteolysis, which can be increased by high insulin in lymphocytes
301 and adipocytes (22,23,65). However, the fold reduction of *Insr* mRNA was smaller than fold
302 reduction of INSR protein in our cell model, suggesting that additional mechanisms may be
303 involved in modulating the protein abundance of INSR. In addition to the downregulation of INSR
304 protein abundance, we found a subtle increase in INSR internalization with, but future studies will
305 be required to determine the role and mechanism of this phenomenon. Interestingly, chick liver
306 cells exposed to 50 nM insulin for 18 h had decreased surface, but unchanged total, INSR with
307 no alteration in INSR protein synthesis and degradation rates, suggesting that the regulation of
308 INSR by hyperinsulinemia may have distinct control mechanisms in certain cell types (20).
309 Despite its inherent reductionism, our *in vitro* model reemphasized the critical role of
310 hyperinsulinemia in the development of insulin resistance and T2D. We demonstrated that *in vitro*
311 hyperinsulinemia and serum fasting have profound effects on AKT and ERK signaling and protein
312 levels, INSR abundance and localization, and transcriptional activities, which provided valuable
313 insights on the molecular mechanisms of insulin resistance. Future additional characterization of
314 the effect of hyperinsulinemism on INSR trafficking, degradation, and detailed post-receptor
315 alterations will provide more insight in the molecular mechanisms of diabetes progression and
316 further highlights dysregulated basal insulin as a direct cause and hallmark of diabetes.
317

318 **Experimental Procedures**

319 ***Cell culture***

320 The C2C12 mouse myoblast (ATCC cell line provided by Dr. Brain Rodrigues, University
321 of British Columbia, Vancouver, Canada) was maintained in Dulbecco's modified Eagle's
322 medium (DMEM, Invitrogen) supplemented with 10% (v/v) fetal bovine serum (FBS, Gibco), and

323 1% penicillin-streptomycin (100 μg/ml; Gibco). For downstream analysis, 8×10^5 cells/well of
324 cells were seeded in 6-well plates and cultured at 37 °C under 5% CO_2. Confluent (90%)
325 myoblasts were differentiated into myotubes by culturing the cells in differentiation medium
326 (DMEM supplemented with 2% horse serum and 1% penicillin-streptomycin) for 10 days. To
327 induce insulin resistance by hyperinsulinemia *in vitro*, C2C12 myotubes were cultured in
328 differentiation medium containing 2 or 200 nM human insulin (Cat.# I9278, Sigma) for 16 hours
329 prior to reaching day 10 (Fig.1A). Insulin concentrations after the 16 h hyperinsulinemia treatment
330 were measured using human insulin RIA kit (Millipore). For serum starvation, myotubes were
331 maintained in serum-free medium (DMEM supplemented with 1% penicillin-streptomycin) for 6
332 hours. All experiments were repeated with biological replicates using cells in different passages.
333

334 ***Experimental Animals***

335 Animal protocols were approved by the University of British Columbia Animal Care
336 Committee. *Ins1*$^{+/+}$;*Ins2*$^{-/-}$ and *Ins1*$^{+/-}$;*Ins2*$^{-/-}$ mice were randomly assigned to be fed *ad libitum*
337 either a high fat diet (Research Diets D12492, 20% protein, 60% fat, 20% carbohydrate content,
338 energy density 5.21Kcal/g, Brunswick, NJ, US) or low fat diet (Research Diets D12450B, 20%
339 protein 10% fat, 70% carbohydrate content, energy density 3.82Kcal/g, Brunswick, NJ, US) for 4
340 weeks starting from 8 weeks old. Blood fasting glucose was measured using OneTouch Ultra2
341 glucose meters (LifeScan Canada Ltd, BC, Canada), and serum fasting insulin were assessed
342 using mouse insulin ELISA kit (Alpco Diagnostics, Salem, NH, USA), following 4-hour fasting.
343

344 ***Western blot analyses***

345 C2C12 myotubes or mice skeletal muscle (gastrocnemius) tissues were sonicated in RIPA
346 buffer (50 mM β-glycerol phosphate, 10 mM HEPES, 1% Triton X-100, 70 mM NaCl, 2 mM EGTA,
347 1 mM Na_3VO_4, and 1 mM NaF) supplemented with complete mini protease inhibitor cocktail
348 (Roche, Laval, QC), and lysates were resolved by SDS-PAGE. Proteins were then transferred to
349 PVDF membranes (BioRad, CA) and probed with antibodies against p-ERK1/2 (Thr202/Tyr204)
350 (1:1000, Cat. #4370), ERK1/2 (1:1000, Cat. #4695), p-AKT (Ser473) (1:1000, Cat. #9271), p-AKT
351 (Thr308) (1:1000, Cat. #9275), AKT (1:1000, Cat. #9272), INSR-β subunit (1:1000, Cat. #3020S),
352 p-INSRβ (Tyr1150/1151) (1:1000, Cat. #3024), FOXO1 (1:1000, Cat. #2880), p-FOXO1 (Thr24)
353 (1:1000, Cat. #9464), all from Cell Signalling (CST), and β-tubulin (1:2000, Cat. #T0198, Sigma).
354 The signals were detected by secondary HRP-conjugated antibodies (Anti-mouse, Cat. #7076;
355 Anti-rabbit, Cat. #7074; CST) and Pierce ECL Western Blotting Substrate (Thermo Fisher
356 Scientific). Protein band intensities were quantified with Image Studio Lite software (LI-COR).
357

358 ***siRNA knockdown in C2C12 myoblasts***

359 All siRNAs are from Thermo Fisher Scientific with the specific Assay IDs as follows: *Foxo1*
360 (MSS226201), *Sin3a* (151684), *Elf1* (157302), *Mxi1* (68202), *Myc* (68302), *Ets1* (101877), *Hcfc1*
361 (158001), *Nrf1* (68266), *Jund* (67635), *Ctcf* (60925), *Max* (155266), *Maz* (501159), Silencer Cy3-
362 labeled Negative Control No.1 siRNA (AM4621). siRNAs were transfected into C2C12 myoblasts
363 using the Lipofectamine RNAiMAX reagent (Invitrogen) according to the manufacturer's
364 instructions with 50 pmol of siRNA and 4 μl of transfection reagent per well of a 12-well plate.
365

366 ***RNA isolation and quantitative real-time PCR analysis***

367 Total RNA was isolated from both control and high insulin-treated C2C12 myotubes before
368 and after serum starvation or C2C12 myoblasts post siRNA transfection using the RNEasy mini
369 kit (Qiagen). cDNA was generated by reverse transcription using qScript cDNA synthesis kit
370 (Quanta Biosciences, Gaithersburg, MD, USA). Transcript levels of target genes in the equal
371 amount of total cDNA were quantified with SYBR green chemistry (Quanta Biosciences) on a
372 StepOnePlus Real-time PCR System (Applied Biosystems). All data were normalized to *Hprt* by
373 the $2^{-\Delta Ct}$ method. The following primers are used in qPCR: *Insr-A/B* forward 5'-
374 TCCTGAAGGAGCTGGAGGAGT-3', *Insr-A* reverse 5'-CTTTCGGGATGGCCTGG-3', *Insr-B*
375 reverse 5'-TTCGGGATGGCCTACTGTC-3' (66); *Insr* (in siRNA experiments) forward 5'-
376 TTTGTCATGGATGGAGGCTA-3' and reverse 5'-CCTCATCTTGGGGTTGAACT-3' (67) *Igf1r*
377 forward 5'-GGCACAACTACTGCTCCAAAGAC-3' and reverse 5'-CTTTATCACCACCACACACT
378 TCTG-3' (66); *Hprt* forward 5'-TCAGTCAACGGGGGACATAAA-3' and reverse 5'-GGGGCTGT
379 ACTGCTTAACCAG-3' (68); *Foxo1* forward 5'-CCCAGGCCGGAGTTTAACC-3' and reverse 5'-
380 GTTGCTCATAAAGTCGGTGCT-3', *Tbp* forward 5'-AGAACAATCCAGACTAGCAGCA-3' and
381 reverse 5'-GGGAACTTCACATCACAGCTC-3', *Nrf1* forward 5'-TATGGCGGAAGTAATGAAAG
382 ACG-3' and reverse 5'-CAACGTAAGCTCTGCCTTGTT-3', *Jund* forward 5'-GAAACGCCCTTCTA
383 TGGCGA-3' and reverse 5'-CAGCGCGTCTTTCTTCAGC-3', *Ctcf* forward 5'-GATCCTACCCTTC
384 TCCAGATGAA-3' and reverse 5'-GTACCGTCACAGGAACAGGT-3', *Mxi1* forward 5'-AACATGG
385 CTACGCCTCATCG-3' and reverse 5'-CGGTTCTTTTCCAACTCATTGTG-3', *Elf1* forward 5'-
386 TGTCCAACAGAACGACCTAGT-3' and reverse 5'-CACACAAGCTAGACCAGCATAA-3', *Ets1*
387 forward 5'-TCCTATCAGCTCGGAAGAACTC-3' and reverse 5'-TCTTGCTTGATGGCAAAGT
388 AGTC-3', *Maz* forward 5'-GCCCCAGTTGCATCTGTCTT-3' and reverse 5'-CTTCGGAGGTTGT
389 AGCCGTT-3', *Max* forward 5'-ACCATAATGCACTGGAACGAAA-3' and reverse 5'-GTCCCGC

390 AAACTGTGAAAGC-3', *Myc* forward 5'-ATGCCCCTCAACGTGAACTTC-3' and reverse 5'-
391 CGCAACATAGGATGGAGAGCA-3', *Hcfc1* forward 5'-CGGCAACGAGGGGATAGTG-3' and
392 reverse 5'-TAGGCGAGTACCATCACACAC-3', *Sin3a* forward 5'-GCCTGTGGAGTTTAATCAT
393 GCC-3' and reverse 5'-CCTCTTGCTCAGTCAAAGCTG-3', *Irs2* forward 5'-CTGCGTCCTCTCC
394 CAAAGTG-3' and reverse 5'-GGGGTCATGGGCATGTAGC-3' (PrimerBank https://pga.mgh.
395 harvard.edu/primerbank/index.html).
396

397 ***Surface Protein Biotinylation Assay***

398 Biotinylation of surface proteins was performed as previously described (69) with
399 modifications (Fig. 4A). In brief, cells were incubated with cell-impermeable EZ-Link-NHS-SS-
400 biotin (300 μg/ml in PBS; Pierce) at 37°C for 2 min. Cells were then immediately placed on ice
401 and washed with ice-cold 50 mM Tris-buffered saline (TBS) to remove excess biotin. For isolating
402 surface proteins, cells were washed using ice-cold PBS and lysed in complete RIPA buffer
403 (supplemented with cOmplete mini protease inhibitor cocktail (Roche, Laval, QC) and Na_3VO_4).
404 For detecting internalized proteins, cells were washed with PBS and incubated in serum-free
405 medium supplemented with 0.2, 2 or 20 nM insulin at 37°C to stimulate INSR internalization. After
406 certain time periods, cells were placed on ice, washed with ice-cold PBS, incubated with
407 Glutathione solution (50 mM glutathione, 75 mM NaCl, 1 mM EDTA, 1% BSA, 75 mM NaOH) for
408 20 min to strip remaining surface biotin, washed with excess PBS, and lysed in complete RIPA
409 buffer. Lysates were quantitated and incubated with NeutrAvidin beads (Pierce) overnight at 4 °C
410 to isolate biotinylated surface or internalized proteins. Biotinylated proteins were eluted from the
411 NeutrAvidin beads by boiling in Blue Loading Buffer (CST) containing 50 mM DTT for 5 min.

412 Surface or internalized INSR in eluent and total INSR in lysates were detected in Western blot
413 analysis.
414
415 ***RNA sequencing and bioinformatic analysis***
416 Total RNA isolated from both control and 200 nM insulin-treated C2C12 myotubes before
417 and after serum starvation (4 groups, n = 5 each group) were sequenced by BRC Sequencing
418 Core at the University of British Columbia. Sample quality control was performed using the Agilent
419 2100 Bioanalyzer. Qualifying samples were then prepped following the standard protocol for the
420 NEBNext Ultra II Stranded mRNA (New England Biolabs). Sequencing was performed on the
421 Illumina NextSeq 500 with Paired End 42bp × 42bp reads. Sequencing data was demultiplexed
422 using Illumina's bcl2fastq2. De-multiplexed read sequences were then aligned to the Mus
423 Musculous mm10 reference sequence using STAR aligner (https://www.ncbi.nlm.nih.gov/
424 pubmed/23104886). Assembly was estimated using Cufflinks (http://cole-trapnell-
425 lab.github.io/cufflinks/) through bioinformatics apps available on Illumina Sequence Hub using
426 default settings. A visual analytic platform NetworkAnalyst 3.0 (http://www.networkanalyst.ca/)
427 was used for PCA, differential expression (DESeq2), PPI network, and TF-gene network analysis.
428 For the transcription factor and gene network, data are derived from the ENCODE ChIP-seq data.
429 PPI network data are based on STRING interactome with high (900-1000) confidence score.
430
431 ***Statistics***
432 Data were presented as mean ± SEM in addition to the individual data points. All data were
433 analyzed using R Studio 3.4.1. A significance level of adjusted $p < 0.05$ was used throughout. All
434 western blot quantifications (protein band intensity) were analyzed using linear regression

435 modeling (70). Linear mixed effect models (R package – lme4) were fitted using restricted
436 maximum likelihood (70,71). Predictor variables were included as fixed effects and sample IDs
437 were included as random effects. Mixed effect modeling was used to account for repeated sample
438 measurements and missing data (70). Where the random effect was not significant, linear fixed
439 effect modeling was used. Heteroscedasticity and normality of residuals were analyzed used
440 Levene's test and the Shapiro–Wilk test, respectively. Predictor variables, insulin treatment
441 (overnight and acute) and time, were treated as ordinal factors and continuous factor, respectively.
442 The outcome variable, protein band intensity, was treated as a continuous factor and log-
443 transformed when residuals are not homoscedastic and/or normally distributed. Multiple
444 comparison p-values were adjusted using the Tukey method.
445

446 **Acknowledgments:** We acknowledge Dr. Brain Rodrigues for providing the C2C12 cells. We
447 thank our colleagues Xiaoke Hu and Leanne Beet for performing the insulin
448 radioimmunoassays. We thank those who provided helpful comments on the drafts of this
449 manuscript posted on *Biorxiv*.
450

451 **Contributions:** HC designed the study, performed all experiments except the high-fat feeding,
452 analyzed data and wrote the manuscript. JDB performed *in vivo* high fat feeding and analyzed
453 the related data. SW performed statistical analysis and edited the manuscript. NN performed
454 siRNA knockdown experiments. JDJ designed the study, supervised the research and edited the
455 manuscript. JDJ is the ultimate guarantor of this work.
456

457 **Funding:** This study was funded by a CIHR Operating Grant to JDJ.

458

459 **Conflict of interest:** The authors declare that they have no conflicts of interest with the contents
460 of this article.

461

462 **References**

463 1. Defronzo, R. A. (2009) Banting Lecture. From the triumvirate to the ominous octet: a new
464 paradigm for the treatment of type 2 diabetes mellitus. *Diabetes* **58**, 773-795
465 2. Prentki, M., and Nolan, C. J. (2006) Islet beta cell failure in type 2 diabetes. *J Clin Invest*
466 **116**, 1802-1812
467 3. Corkey, B. E. (2012) Banting lecture 2011: hyperinsulinemia: cause or consequence?
468 *Diabetes* **61**, 4-13
469 4. Shanik, M. H., Xu, Y., Skrha, J., Dankner, R., Zick, Y., and Roth, J. (2008) Insulin resistance
470 and hyperinsulinemia: is hyperinsulinemia the cart or the horse? *Diabetes Care* **31 Suppl 2**,
471 S262-268
472 5. Page, M. M., and Johnson, J. D. (2018) Mild Suppression of Hyperinsulinemia to Treat
473 Obesity and Insulin Resistance. *Trends Endocrinol Metab* **29**, 389-399
474 6. Le Stunff, C., and Bougneres, P. (1994) Early changes in postprandial insulin secretion, not
475 in insulin sensitivity, characterize juvenile obesity. *Diabetes* **43**, 696-702
476 7. Spadaro, L., Alagona, C., Palermo, F., Piro, S., Calanna, S., Parrinello, G., Purrello, F., and
477 Rabuazzo, A. M. (2011) Early phase insulin secretion is increased in subjects with normal
478 fasting glucose and metabolic syndrome: a premature feature of beta-cell dysfunction. *Nutr*
479 *Metab Cardiovasc Dis* **21**, 206-212
480 8. Trico, D., Natali, A., Arslanian, S., Mari, A., and Ferrannini, E. (2018) Identification,
481 pathophysiology, and clinical implications of primary insulin hypersecretion in nondiabetic
482 adults and adolescents. *JCI Insight* **3**
483 9. Dankner, R., Chetrit, A., Shanik, M. H., Raz, I., and Roth, J. (2012) Basal state
484 hyperinsulinemia in healthy normoglycemic adults heralds dysglycemia after more than two
485 decades of follow up. *Diabetes Metab Res Rev* **28**, 618-624
486 10. Zimmet, P. Z., Collins, V. R., Dowse, G. K., and Knight, L. T. (1992) Hyperinsulinaemia in
487 youth is a predictor of type 2 (non-insulin-dependent) diabetes mellitus. *Diabetologia* **35**,
488 534-541

489 11. Templeman, N. M., Flibotte, S., Chik, J. H. L., Sinha, S., Lim, G. E., Foster, L. J., Nislow, C.,
490 and Johnson, J. D. (2017) Reduced Circulating Insulin Enhances Insulin Sensitivity in Old
491 Mice and Extends Lifespan. *Cell Rep* **20**, 451-463
492 12. Mehran, A. E., Templeman, N. M., Brigidi, G. S., Lim, G. E., Chu, K. Y., Hu, X., Botezelli, J.
493 D., Asadi, A., Hoffman, B. G., Kieffer, T. J., Bamji, S. X., Clee, S. M., and Johnson, J. D.
494 (2012) Hyperinsulinemia drives diet-induced obesity independently of brain insulin
495 production. *Cell Metab* **16**, 723-737
496 13. Page, M. M., Skovso, S., Cen, H., Chiu, A. P., Dionne, D. A., Hutchinson, D. F., Lim, G. E.,
497 Szabat, M., Flibotte, S., Sinha, S., Nislow, C., Rodrigues, B., and Johnson, J. D. (2018)
498 Reducing insulin via conditional partial gene ablation in adults reverses diet-induced weight
499 gain. *FASEB J* **32**, 1196-1206
500 14. Hamza, S. M., Sung, M. M., Gao, F., Soltys, C. M., Smith, N. P., MacDonald, P. E., Light, P.
501 E., and Dyck, J. R. (2017) Chronic insulin infusion induces reversible glucose intolerance in
502 lean rats yet ameliorates glucose intolerance in obese rats. *Biochim Biophys Acta Gen Subj*
503 **1861**, 313-322
504 15. Yang, X., Mei, S., Gu, H., Guo, H., Zha, L., Cai, J., Li, X., Liu, Z., and Cao, W. (2014)
505 Exposure to excess insulin (glargine) induces type 2 diabetes mellitus in mice fed on a
506 chow diet. *J Endocrinol* **221**, 469-480
507 16. Marangou, A. G., Weber, K. M., Boston, R. C., Aitken, P. M., Heggie, J. C., Kirsner, R. L.,
508 Best, J. D., and Alford, F. P. (1986) Metabolic consequences of prolonged hyperinsulinemia
509 in humans. Evidence for induction of insulin insensitivity. *Diabetes* **35**, 1383-1389
510 17. Del Prato, S., Leonetti, F., Simonson, D. C., Sheehan, P., Matsuda, M., and DeFronzo, R. A.
511 (1994) Effect of sustained physiologic hyperinsulinaemia and hyperglycaemia on insulin
512 secretion and insulin sensitivity in man. *Diabetologia* **37**, 1025-1035
513 18. Gregory, J. M., Smith, T. J., Slaughter, J. C., Mason, H. R., Hughey, C. C., Smith, M. S.,
514 Kandasamy, B., Greeley, S. A. W., Philipson, L. H., Naylor, R. N., Letourneau, L. R.,
515 Abumrad, N. N., Cherrington, A. D., and Moore, D. J. (2019) Iatrogenic Hyperinsulinemia,
516 Not Hyperglycemia, Drives Insulin Resistance in Type 1 Diabetes as Revealed by
517 Comparison to GCK-MODY (MODY2). *Diabetes*
518 19. Soll, A. H., Kahn, C. R., and Neville, D. M. (1975) Insulin binding to liver plasm membranes
519 in the obese hyperglycemic (ob/ob) mouse. Demonstration of a decreased number of
520 functionally normal receptors. *J Biol Chem* **250**, 4702-4707
521 20. Krupp, M., and Lane, M. D. (1981) On the mechanism of ligand-induced down-regulation of
522 insulin receptor level in the liver cell. *J Biol Chem* **256**, 1689-1694

523 21. Garvey, W. T., Olefsky, J. M., and Marshall, S. (1985) Insulin receptor down-regulation is
524 linked to an insulin-induced postreceptor defect in the glucose transport system in rat
525 adipocytes. *J Clin Invest* **76**, 22-30
526 22. Okabayashi, Y., Maddux, B. A., McDonald, A. R., Logsdon, C. D., Williams, J. A., and
527 Goldfine, I. D. (1989) Mechanisms of insulin-induced insulin-receptor downregulation.
528 Decrease of receptor biosynthesis and mRNA levels. *Diabetes* **38**, 182-187
529 23. Ronnett, G. V., Knutson, V. P., and Lane, M. D. (1982) Insulin-induced down-regulation of
530 insulin receptors in 3T3-L1 adipocytes. Altered rate of receptor inactivation. *J Biol Chem*
531 **257**, 4285-4291
532 24. Gavin, J. R., Roth, J., Neville, D. M., de Meyts, P., and Buell, D. N. (1974) Insulin-
533 dependent regulation of insulin receptor concentrations: a direct demonstration in cell
534 culture. *Proc Natl Acad Sci U S A* **71**, 84-88
535 25. Melmed, S., Polonsky, K. S., Larsen, P. R., and Kronenberg, H. M. (2017) *Williams*
536 *Textbook of Endocrinology*, 13th ed., Elsevier
537 Saunders
538 26. Boucher, J., Kleinridders, A., and Kahn, C. R. (2014) Insulin receptor signaling in normal
539 and insulin-resistant states. *Cold Spring Harb Perspect Biol* **6**
540 27. Fröjdö, S., Vidal, H., and Pirola, L. (2009) Alterations of insulin signaling in type 2 diabetes:
541 a review of the current evidence from humans. *Biochim Biophys Acta* **1792**, 83-92
542 28. Morikawa, Y., Ueyama, E., and Senba, E. (2004) Fasting-induced activation of mitogen-
543 activated protein kinases (ERK/p38) in the mouse hypothalamus. *J Neuroendocrinol* **16**,
544 105-112
545 29. Jochen, A. L., Berhanu, P., and Olefsky, J. M. (1986) Insulin Internalization and Degradation
546 in Adipocytes from Normal and Type-Ii Diabetic Subjects. *J Clin Endocr Metab* **62**, 268-274
547 30. Trischitta, V., Gullo, D., Squatrito, S., Pezzino, V., Goldfine, I. D., and Vigneri, R. (1986)
548 Insulin Internalization into Monocytes Is Decreased in Patients with Type-Ii Diabetes-
549 Mellitus. *J Clin Endocr Metab* **62**, 522-528
550 31. El Akoum, S., Lamontagne, V., Cloutier, I., and Tanguay, J. F. (2011) Nature of fatty acids in
551 high fat diets differentially delineates obesity-linked metabolic syndrome components in
552 male and female C57BL/6J mice. *Diabetol Metab Syndr* **3**
553 32. Sbraccia, P., D'Adamo, M., Leonetti, F., Caiola, S., Iozzo, P., Giaccari, A., Buongiorno, A.,
554 and Tamburrano, G. (1996) Chronic primary hyperinsulinaemia is associated with altered
555 insulin receptor mRNA splicing in muscle of patients with insulinoma. *Diabetologia* **39**, 220-
556 225

557 33. Orengo, D. J., Aguadé, M., and Juan, E. (2017) Characterization of dFOXO binding sites
558 upstream of the Insulin Receptor P2 promoter across the Drosophila phylogeny. *Plos One*
559 **12**, e0188357
560 34. Puig, O., and Tjian, R. (2005) Transcriptional feedback control of insulin receptor by
561 dFOXO/FOXO1. *Genes Dev* **19**, 2435-2446
562 35. Ni, Y. G., Wang, N., Cao, D. J., Sachan, N., Morris, D. J., Gerard, R. D., Kuro-O, M.,
563 Rothermel, B. A., and Hill, J. A. (2007) FoxO transcription factors activate Akt and attenuate
564 insulin signaling in heart by inhibiting protein phosphatases. *Proc Natl Acad Sci U S A* **104**,
565 20517-20522
566 36. Nakae, J., Kitamura, T., Ogawa, W., Kasuga, M., and Accili, D. (2001) Insulin regulation of
567 gene expression through the forkhead transcription factor Foxo1 (Fkhr) requires kinases
568 distinct from Akt. *Biochemistry* **40**, 11768-11776
569 37. Kubota, T., Inoue, M., Kubota, N., Takamoto, I., Mineyama, T., Iwayama, K., Tokuyama, K.,
570 Moroi, M., Ueki, K., Yamauchi, T., and Kadowaki, T. (2018) Downregulation of macrophage
571 Irs2 by hyperinsulinemia impairs IL-4-indeuced M2a-subtype macrophage activation in
572 obesity. *Nat Commun* **9**, 4863
573 38. Pirola, L., Bonnafous, S., Johnston, A. M., Chaussade, C., Portis, F., and Van Obberghen,
574 E. (2003) Phosphoinositide 3-kinase-mediated reduction of insulin receptor substrate-1/2
575 protein expression via different mechanisms contributes to the insulin-induced
576 desensitization of its signaling pathways in L6 muscle cells. *J Biol Chem* **278**, 15641-15651
577 39. Rachdaoui, N., Polo-Parada, L., and Ismail-Beigi, F. (2019) Prolonged Exposure to Insulin
578 Inactivates Akt and Erk1/2 and Increases Pancreatic Islet and INS1E beta-Cell Apoptosis. *J*
579 *Endocr Soc* **3**, 69-90
580 40. Lim, G. E., Huang, G. J., Flora, N., LeRoith, D., Rhodes, C. J., and Brubaker, P. L. (2009)
581 Insulin regulates glucagon-like peptide-1 secretion from the enteroendocrine L cell.
582 *Endocrinology* **150**, 580-591
583 41. Turner, M. C., Martin, N. R. W., Player, D. J., Ferguson, R. A., Wheeler, P., Green, C. J. Z.,
584 Akam, E. C., and Lewis, M. P. (2020) Characterising hyperinsulinaemia induced insulin
585 resistance in human skeletal muscle cells. *J Mol Endocrinol*
586 42. Kahn, C. R. (1978) Insulin resistance, insulin insensitivity, and insulin unresponsiveness: a
587 necessary distinction. *Metabolism* **27**, 1893-1902
588 43. Adachi, M., Katsumura, K. R., Fujii, K., Kobayashi, S., Aoki, H., and Matsuzaki, M. (2003)
589 Proteasome-dependent decrease in Akt by growth factors in vascular smooth muscle cells.
590 *FEBS Lett* **554**, 77-80

591 44. Kim, B., McLean, L. L., Philip, S. S., and Feldman, E. L. (2011) Hyperinsulinemia induces
592 insulin resistance in dorsal root ganglion neurons. *Endocrinology* **152**, 3638-3647
593 45. Liu, H. Y., Hong, T., Wen, G. B., Han, J., Zuo, D., Liu, Z., and Cao, W. (2009) Increased
594 basal level of Akt-dependent insulin signaling may be responsible for the development of
595 insulin resistance. *Am J Physiol Endocrinol Metab* **297**, E898-906
596 46. Zhang, Z., Li, X., Liu, G., Gao, L., Guo, C., Kong, T., Wang, H., Gao, R., Wang, Z., and Zhu,
597 X. (2011) High insulin concentrations repress insulin receptor gene expression in calf
598 hepatocytes cultured in vitro. *Cell Physiol Biochem* **27**, 637-640
599 47. Palsgaard, J., Brøns, C., Friedrichsen, M., Dominguez, H., Jensen, M., Storgaard, H.,
600 Spohr, C., Torp-Pedersen, C., Borup, R., De Meyts, P., and Vaag, A. (2009) Gene
601 expression in skeletal muscle biopsies from people with type 2 diabetes and relatives:
602 differential regulation of insulin signaling pathways. *Plos One* **4**, e6575
603 48. Martinez, S. C., Cras-Méneur, C., Bernal-Mizrachi, E., and Permutt, M. A. (2006) Glucose
604 regulates Foxo1 through insulin receptor signaling in the pancreatic islet beta-cell. *Diabetes*
605 **55**, 1581-1591
606 49. Briata, P., Briata, L., and Gherzi, R. (1990) Glucose starvation and glycosylation inhibitors
607 reduce insulin receptor gene expression: characterization and potential mechanism in
608 human cells. *Biochem Biophys Res Commun* **169**, 397-405
609 50. Liu, H. Y., Cao, S. Y., Hong, T., Han, J., Liu, Z., and Cao, W. (2009) Insulin is a stronger
610 inducer of insulin resistance than hyperglycemia in mice with type 1 diabetes mellitus
611 (T1DM). *J Biol Chem* **284**, 27090-27100
612 51. Ciaraldi, T. P., Abrams, L., Nikoulina, S., Mudaliar, S., and Henry, R. R. (1995) Glucose
613 transport in cultured human skeletal muscle cells. Regulation by insulin and glucose in
614 nondiabetic and non-insulin-dependent diabetes mellitus subjects. *J Clin Invest* **96**, 2820-
615 2827
616 52. Mattson, M. P., Longo, V. D., and Harvie, M. (2017) Impact of intermittent fasting on health
617 and disease processes. *Ageing Res Rev* **39**, 46-58
618 53. Patterson, R. E., and Sears, D. D. (2017) Metabolic Effects of Intermittent Fasting. *Annu*
619 *Rev Nutr* **37**, 371-393
620 54. Nuttall, F. Q., Almokayyad, R. M., and Gannon, M. C. (2015) Comparison of a
621 carbohydrate-free diet vs. fasting on plasma glucose, insulin and glucagon in type 2
622 diabetes. *Metabolism* **64**, 253-262
623 55. Sutton, E. F., Beyl, R., Early, K. S., Cefalu, W. T., Ravussin, E., and Peterson, C. M. (2018)
624 Early Time-Restricted Feeding Improves Insulin Sensitivity, Blood Pressure, and Oxidative

625 Stress Even without Weight Loss in Men with Prediabetes. *Cell Metab* **27**, 1212-1221
626 e1213
627 56. Williams, K. V., Mullen, M. L., Kelley, D. E., and Wing, R. R. (1998) The effect of short
628 periods of caloric restriction on weight loss and glycemic control in type 2 diabetes.
629 *Diabetes Care* **21**, 2-8
630 57. Foti, D., Iuliano, R., Chiefari, E., and Brunetti, A. (2003) A nucleoprotein complex containing
631 Sp1, C/EBP beta, and HMGI-Y controls human insulin receptor gene transcription. *Mol Cell*
632 *Biol* **23**, 2720-2732
633 58. Foti, D., Chiefari, E., Fedele, M., Iuliano, R., Brunetti, L., Paonessa, F., Manfioletti, G.,
634 Barbetti, F., Brunetti, A., Croce, C. M., and Fusco, A. (2005) Lack of the architectural factor
635 HMGA1 causes insulin resistance and diabetes in humans and mice. *Nat Med* **11**, 765-773
636 59. Qiu, B., Shi, X., Wong, E. T., Lim, J., Bezzi, M., Low, D., Zhou, Q., Akıncılar, S. C.,
637 Lakshmanan, M., Swa, H. L., Tham, J. M., Gunaratne, J., Cheng, K. K., Hong, W., Lam, K.
638 S., Ikawa, M., Guccione, E., Xu, A., Han, W., and Tergaonkar, V. (2014) NUCKS is a
639 positive transcriptional regulator of insulin signaling. *Cell Rep* **7**, 1876-1886
640 60. Kadamb, R., Mittal, S., Bansal, N., Batra, H., and Saluja, D. (2013) Sin3: insight into its
641 transcription regulatory functions. *Eur J Cell Biol* **92**, 237-246
642 61. Nascimento, E. M., Cox, C. L., MacArthur, S., Hussain, S., Trotter, M., Blanco, S., Suraj, M.,
643 Nichols, J., Kübler, B., Benitah, S. A., Hendrich, B., Odom, D. T., and Frye, M. (2011) The
644 opposing transcriptional functions of Sin3a and c-Myc are required to maintain tissue
645 homeostasis. *Nat Cell Biol* **13**, 1395-1405
646 62. Zervos, A. S., Gyuris, J., and Brent, R. (1993) Mxi1, a protein that specifically interacts with
647 Max to bind Myc-Max recognition sites. *Cell* **72**, 223-232
648 63. Langlet, F., Haeusler, R. A., Lindén, D., Ericson, E., Norris, T., Johansson, A., Cook, J. R.,
649 Aizawa, K., Wang, L., Buettner, C., and Accili, D. (2017) Selective Inhibition of FOXO1
650 Activator/Repressor Balance Modulates Hepatic Glucose Handling. *Cell* **171**, 824-835.e818
651 64. Sumitani, S., Goya, K., Testa, J. R., Kouhara, H., and Kasayama, S. (2002) Akt1 and Akt2
652 differently regulate muscle creatine kinase and myogenin gene transcription in insulin-
653 induced differentiation of C2C12 myoblasts. *Endocrinology* **143**, 820-828
654 65. Mayer, C. M., and Belsham, D. D. (2010) Central insulin signaling is attenuated by long-
655 term insulin exposure via insulin receptor substrate-1 serine phosphorylation, proteasomal
656 degradation, and lysosomal insulin receptor degradation. *Endocrinology* **151**, 75-84
657 66. Rowzee, A. M., Ludwig, D. L., and Wood, T. L. (2009) Insulin-like growth factor type 1
658 receptor and insulin receptor isoform expression and signaling in mammary epithelial cells.
659 *Endocrinology* **150**, 3611-3619

660 67. Harith, H. H., Di Bartolo, B. A., Cartland, S. P., Genner, S., and Kavurma, M. M. (2016)
661 Insulin promotes vascular smooth muscle cell proliferation and apoptosis via differential
662 regulation of tumor necrosis factor-related apoptosis-inducing ligand. *J Diabetes* **8**, 568-578
663 68. Zhang, J., Tang, H., Zhang, Y., Deng, R., Shao, L., Liu, Y., Li, F., Wang, X., and Zhou, L.
664 (2014) Identification of suitable reference genes for quantitative RT-PCR during 3T3-L1
665 adipocyte differentiation. *Int J Mol Med* **33**, 1209-1218
666 69. Tseng, L. T., Lin, C. L., Tzen, K. Y., Chang, S. C., and Chang, M. F. (2013) LMBD1 protein
667 serves as a specific adaptor for insulin receptor internalization. *J Biol Chem* **288**, 32424-
668 32432
669 70. Harrison, X. A., Donaldson, L., Correa-Cano, M. E., Evans, J., Fisher, D. N., Goodwin, C. E.
670 D., Robinson, B. S., Hodgson, D. J., and Inger, R. (2018) A brief introduction to mixed
671 effects modelling and multi-model inference in ecology. *PeerJ* **6**, e4794
672 71. Bates, D., Machler, M., Bolker, B. M., and Walker, S. C. (2015) Fitting Linear Mixed-Effects
673 Models Using lme4. *J Stat Softw* **67**, 1-48

674

675

676

677

678

679

680

681

682

683

684

685

686

687

688 **Figure Legends**

689

690 **Figure 1. Basal and acute insulin signaling in an *in vitro* model of hyperinsulinemia-**
691 **induced insulin resistance. (A)** The workflow of C2C12 myotube differentiation, high insulin
692 treatment and serum starvation. Differentiated myotubes were cultured in control (0 nM insulin)
693 or hyperinsulinemic (2 or 200 nM insulin) medium for 16 hours and were analyzed before and
694 after serum starvation. **(A')** The insulin concentration in the medium at the end of 16-hour high
695 insulin treatment (n=3). **(B)** Representative western blot images of phospho-AKT (T308, S473),
696 total AKT, phospho-ERK1/2, and total ERK1/2. **(C)** Total AKT and **(D)** total ERK abundance under
697 high insulin treatments before starvation (BS) and after starvation (AS). **(E)** phospho-AKT (T308,
698 S473) and **(F)** phospho-ERK1/2 measurements before starvation (BS), after starvation (AS), and
699 stimulated by 0.2 or 2 nM insulin for 10 min after serum starvation. (n=6-9; # effect of
700 hyperinsulinemia, $ effect of starvation, & effect of acute insulin, × interaction between two factors,
701 Mixed Effect Model.)

702

703 **Figure 2. Insulin dose- and time-depend acute insulin signaling in a hyperinsulinemia-**
704 **induced insulin resistance model.** Myotubes cultured in control (0 nM insulin) or
705 hyperinsulinemic (200 nM insulin) medium were stimulated with acute 0.2, 2 or 20 nM insulin for
706 1, 5, 10, 15 or 30 min after serum starvation. **(A)** phospho-AKT (T308, S473) and **(B)** phospho-
707 ERK1/2 was measured. (n=4; # effect of hyperinsulinemia, & effect of acute insulin, × interaction
708 between two factors, Mixed Effect Model.)

709

710 **Figure 3. Effects of hyperinsulinemia and serum starvation on INSR protein abundance**
711 **and phosphorylation. (A)** Representative western blot images of phospho-INSR (Y1150/1151)
712 and total INSR. **(B)** The level of total INSR protein before or after serum starvation (n=4-6). **(C)**
713 phospho-INSR (T308, S473) measurements before starvation (BS), after starvation (AS), and
714 stimulated by 0.2 or 2 nM insulin for 10 min after serum starvation (n=4-6). **(D)** Insulin dose- and
715 time-dependent INSR phosphorylation after serum starvation (n=4). (# effect of hyperinsulinemia,
716 $ effect of starvation, & effect of acute insulin, × interaction between two factors, mixed effect
717 model.)
718
719 **Figure 4. Effects of *in vitro* hyperinsulinemia on INSR internalization. (A)** Scheme of surface
720 biotinylation assay to measure surface or internalized INSR. Internalized INSR in isolated proteins
721 is detected by western blots. **(B)** The ratio of surface to total INSR ((n = 3 in BS group, n = 10 in
722 AS group). **(C)** The ratio of internalized to total INSR (n = 4). (# effect of hyperinsulinemia, $ effect
723 of starvation, × interaction between two factors, mixed effect model).
724
725 **Figure 5. *In vivo* correlation between INSR abundance and fasting insulin or glucose in**
726 **mouse skeletal muscle. (A)** INSR and fasting insulin in LFD-fed mice. **(B)** INSR and fasting
727 glucose in LFD-fed mice. **(C)** INSR and fasting insulin in HFD-fed mice. **(D)** INSR and fasting
728 glucose in HFD-fed mice. (n = 7-11)
729
730 **Figure 6. Effects of prolonged hyperinsulinemia and starvation on *Insr* transcription and**
731 **FOXO1 phosphorylation *in vitro*. (A)** The mRNA levels of *Insr* isoform A or B *(Insr-A or B)* before
732 and after starvation (BS and AS) assessed by qPCR. **(B)** *Igf1r* mRNA level. **(C)** The ratio of *Insr-*

733 *A* to *Insr-B* mRNA (n=5). **(D)** Total and T24 phosphorylation of FOXO1 (n = 3 in BS group, n = 10
734 in AS group). ($^{\#}$ effect of hyperinsulinemia, $^{\$}$ effect of starvation, × interaction between two factors,
735 mixed effect model).
736
737 **Figure 7. Transcriptomic analysis of hyperinsulinemia and serum starvation. (A)** Principle
738 component analysis (PCA) of RNA-seq data from 4 groups of treatments, including 0 nM or 200
739 nM prolonged insulin both before and after serum starvation. **(B)** Top 50 differentially expressed
740 genes that have highest adjusted p value and more than 2-fold changes in nested comparisons
741 for the effects of hyperinsulinemia before and after serum starvation. **(C)** Top 20 KEGG pathways
742 enriched among downregulated genes by hyperinsulinemia before starvation (BS, 0 vs 200 nM
743 insulin). The direction of change of the same pathways affected by starvation (200 nM, BS vs AS)
744 or after starvation (AS, 0 vs 200 nM) are also shown. **(D)** Insulin signaling, and **(E)** FOXO signaling
745 pathways enriched in the PPI network of deferentially expressed genes.
746
747 **Figure 8. Identification of upstream transcription factors mediating the overall**
748 **transcriptomic changes and insulin receptor expression. (A)** TF-gene network predicted
749 upstream transcriptional regulators of differentially expressed genes by hyperinsulinemia before
750 starvation. **(B)** Common TFs between the top 30 TF nodes from (A) and key genes in insulin
751 signaling pathways that are downregulated by hyperinsulinemia. TFs upregulated by
752 hyperinsulinemia are in red. **(C)** mRNA levels of the common TFs in (B) after siRNA knockdown.
753 **(D)** The effects of each siRNA knockdown on *Insr* and *Irs2* mRNA levels. (n=4; * $p<0.05$, 1-
754 ANOVA followed by Dunnett multiple comparison test against si*Control*). **(E)** Graphic summary of
755 our current model. Hyperinsulinemia induced sustained phosphorylation of INSR and AKT, which

756 resulted in the inhibition of FOXO1 leading to reduced *Insr* transcription. Dowregulated INSR and
757 post receptor components resulted in reduced insulin signaling upon acute insulin stimulation.
758 SIN3A, which was upregulated by hyperinsulinemia, might repress *Insr* transcription.
759

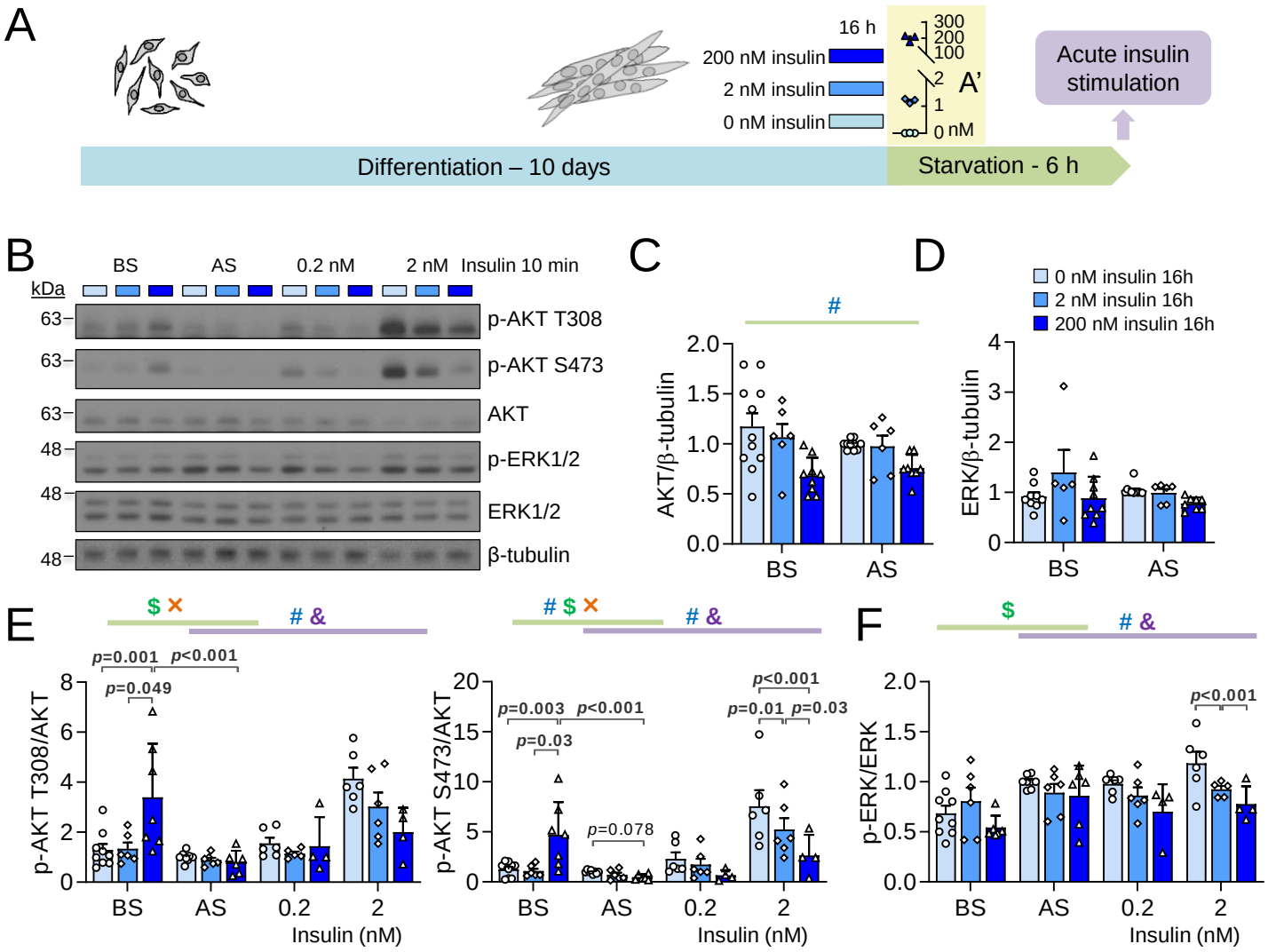

Figure 1. Basal and acute insulin signaling in an *in vitro* hyperinsulinemia-induced insulin resistance model.

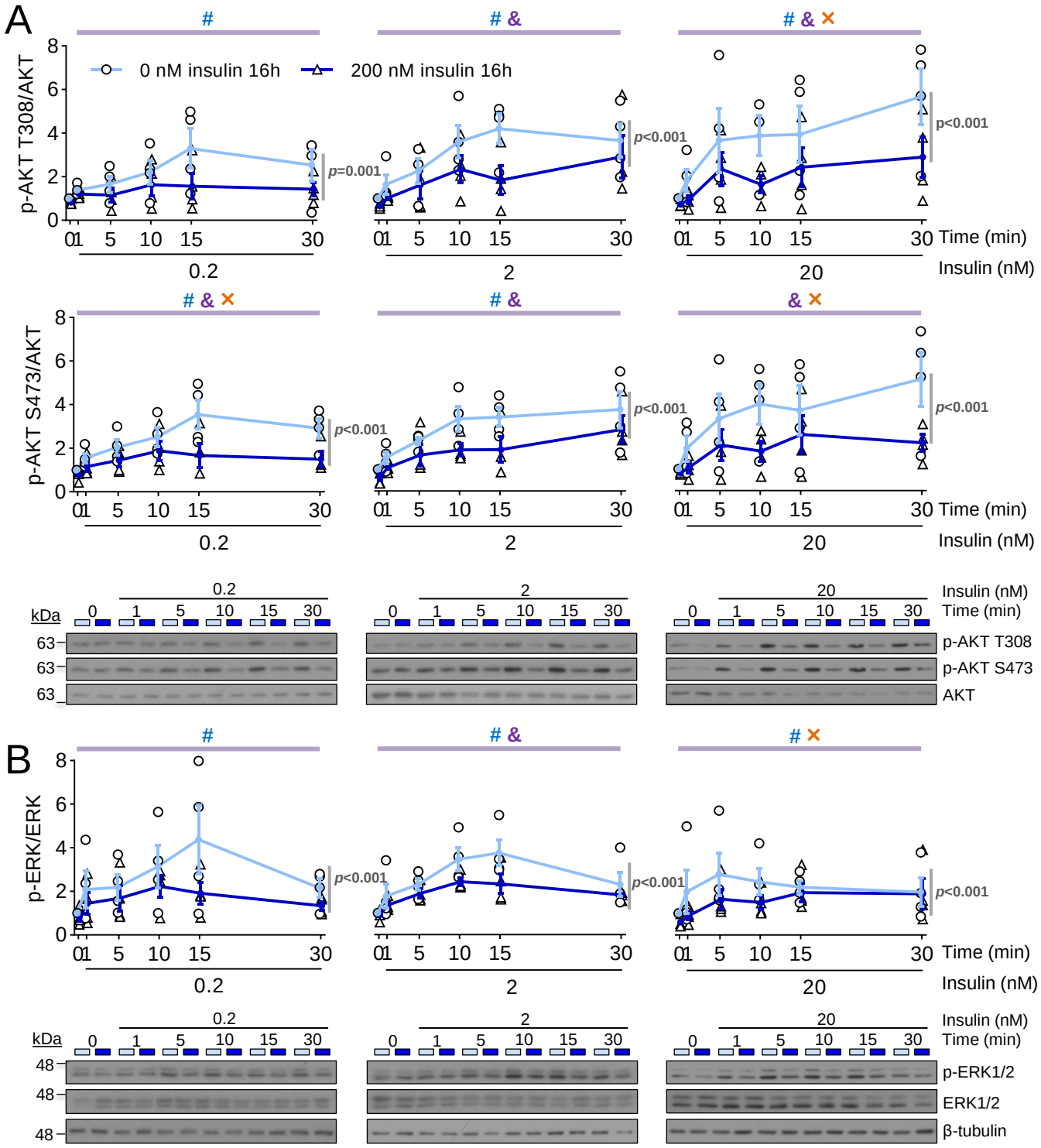

Figure 2. Insulin dose- and time-depend acute insulin signaling in the hyperinsulinemia-induced insulin resistance model.

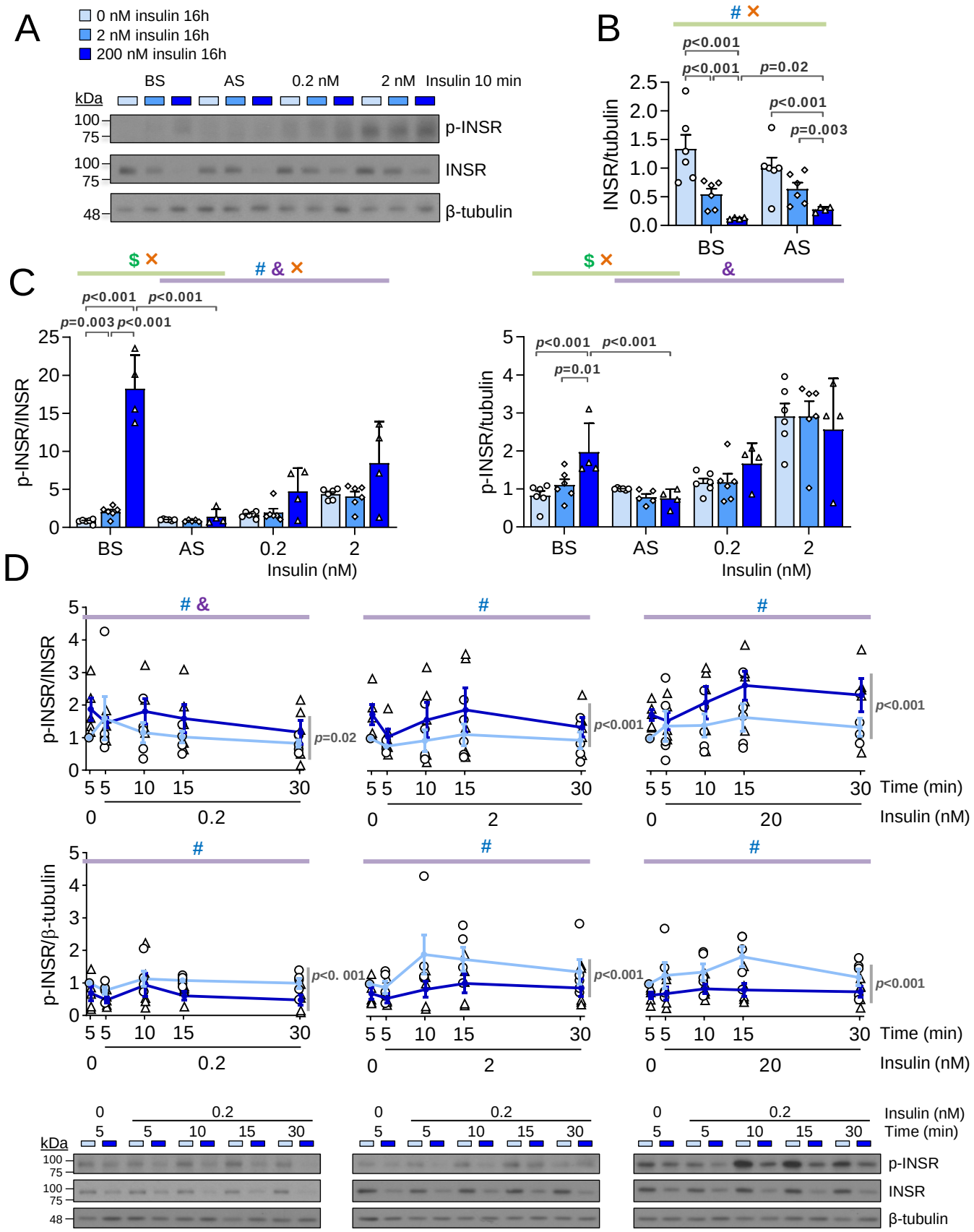

Figure 3. Effects of hyperinsulinemia and serum starvation on INSR abundance and phosphorylation .

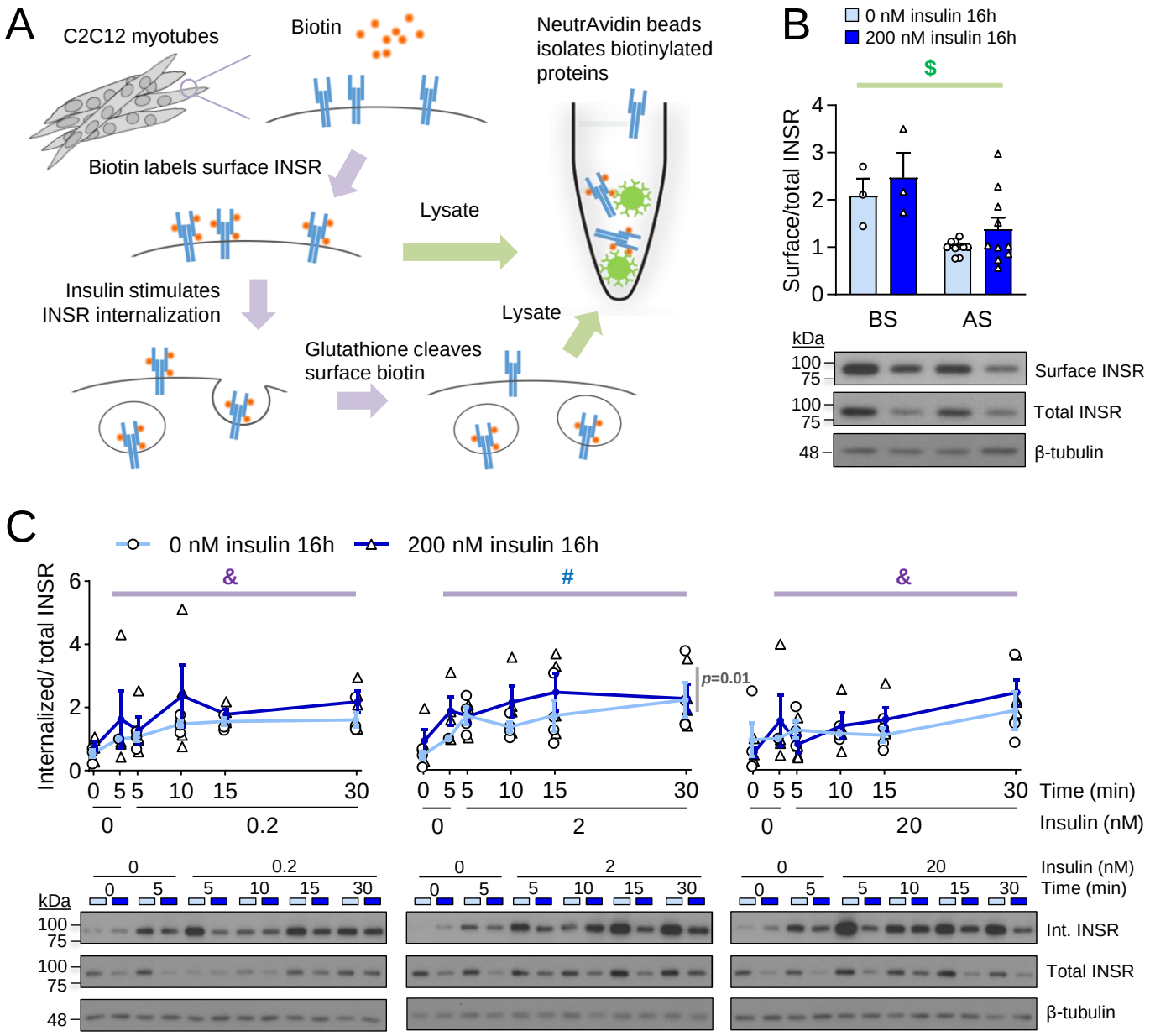

Figure 4. Effects of *in vitro* hyperinsulinemia on INSR internalization.

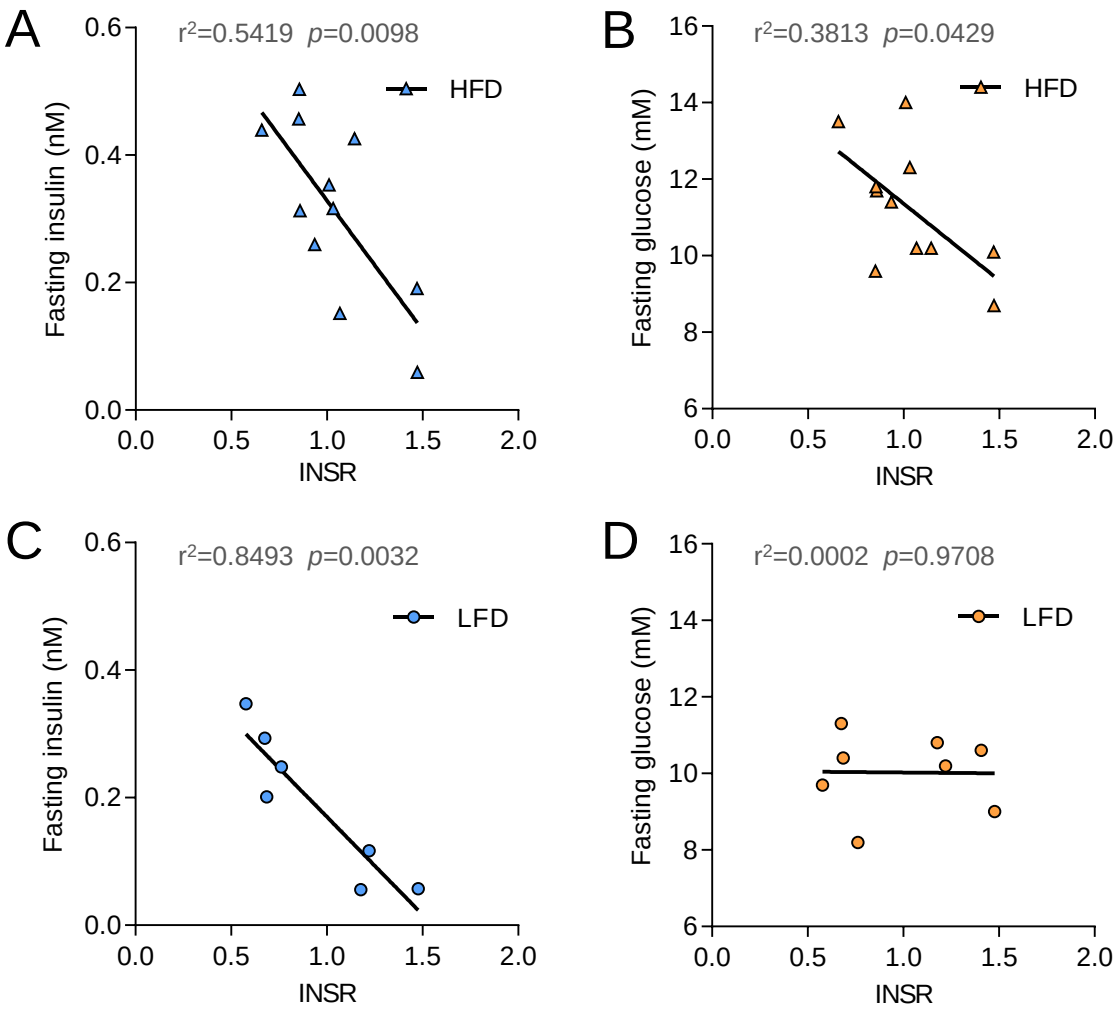

Figure 5. ***In vivo*** **correlation between INSR abundance and fasting insulin or glucose in mouse skeletal muscle.**

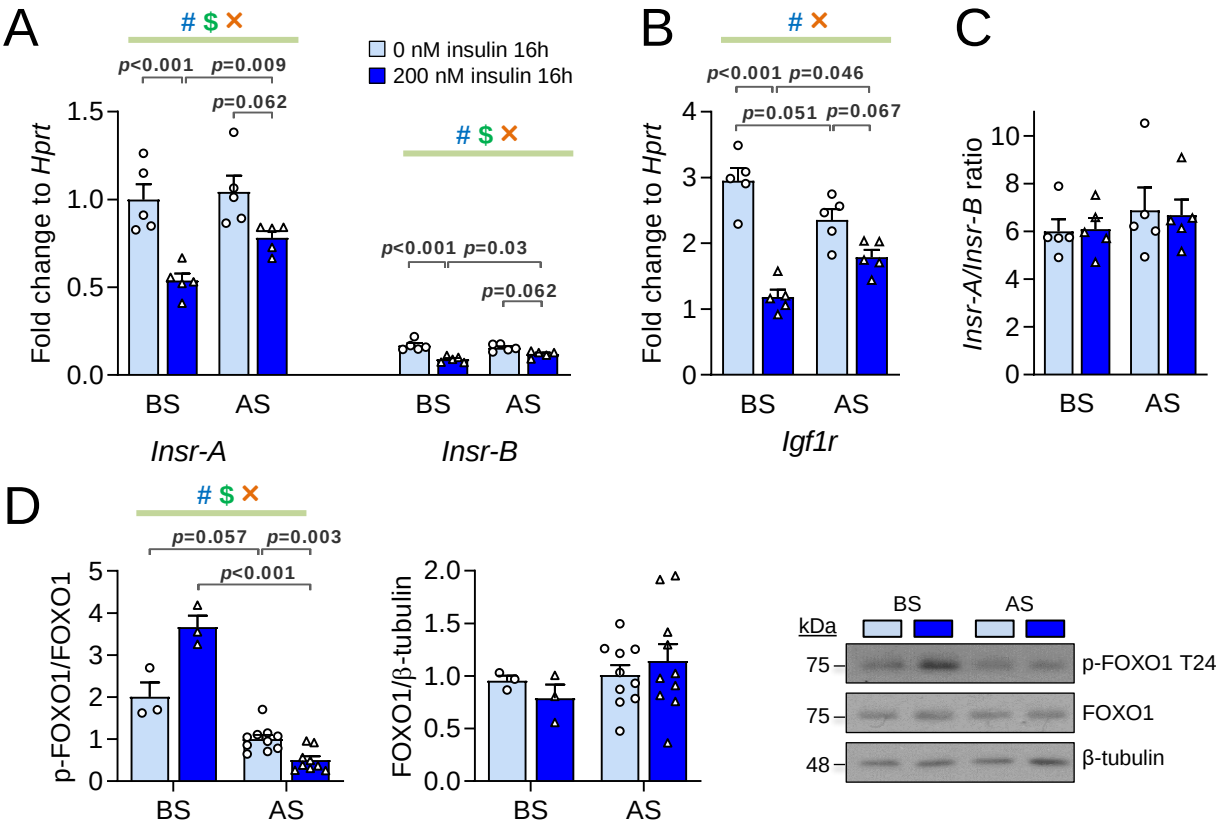

Figure 6. Effects of prolonged hyperinsulinemia and starvation on *Insr* transcription and FOXO1 phosphorylation *in vitro*.

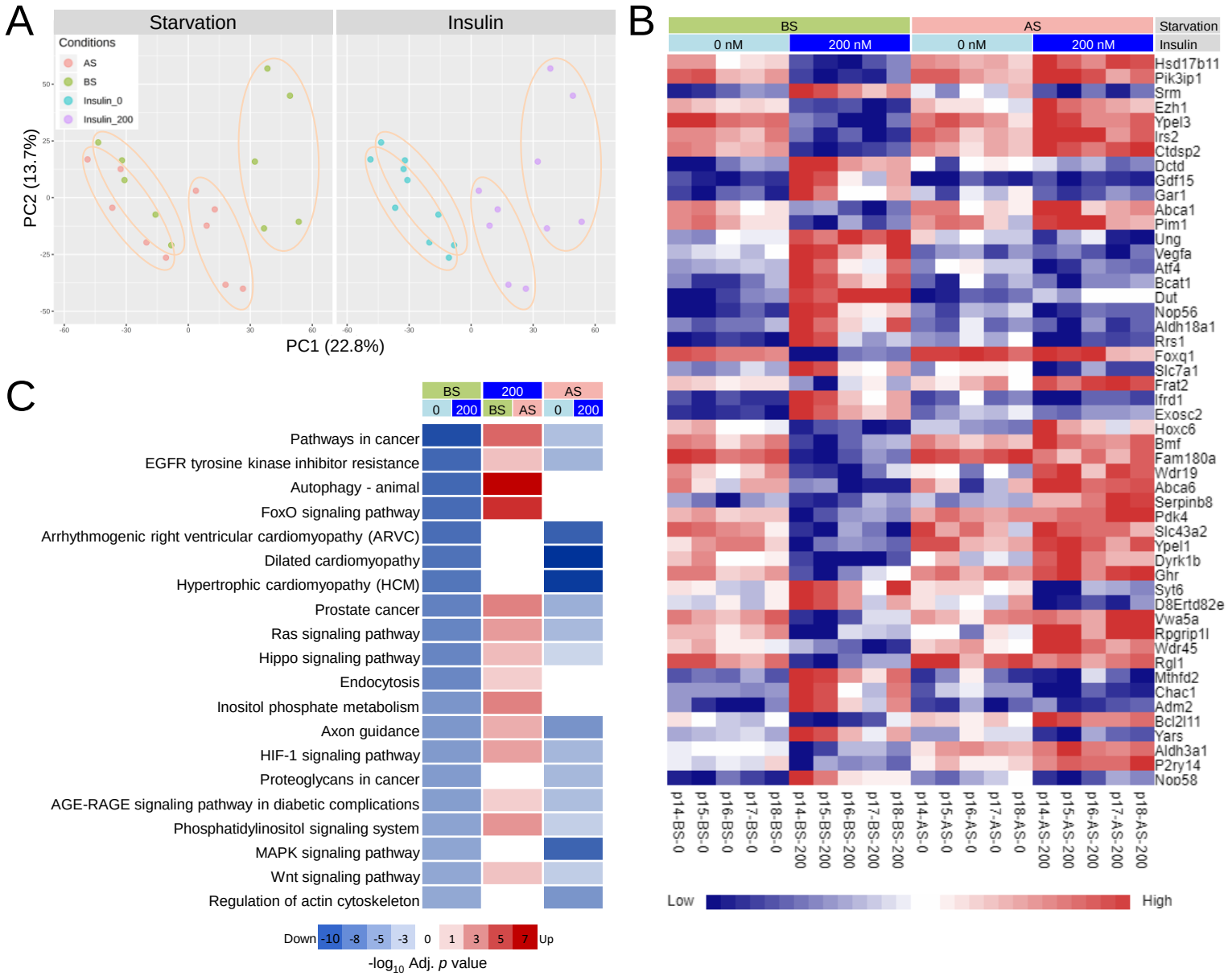

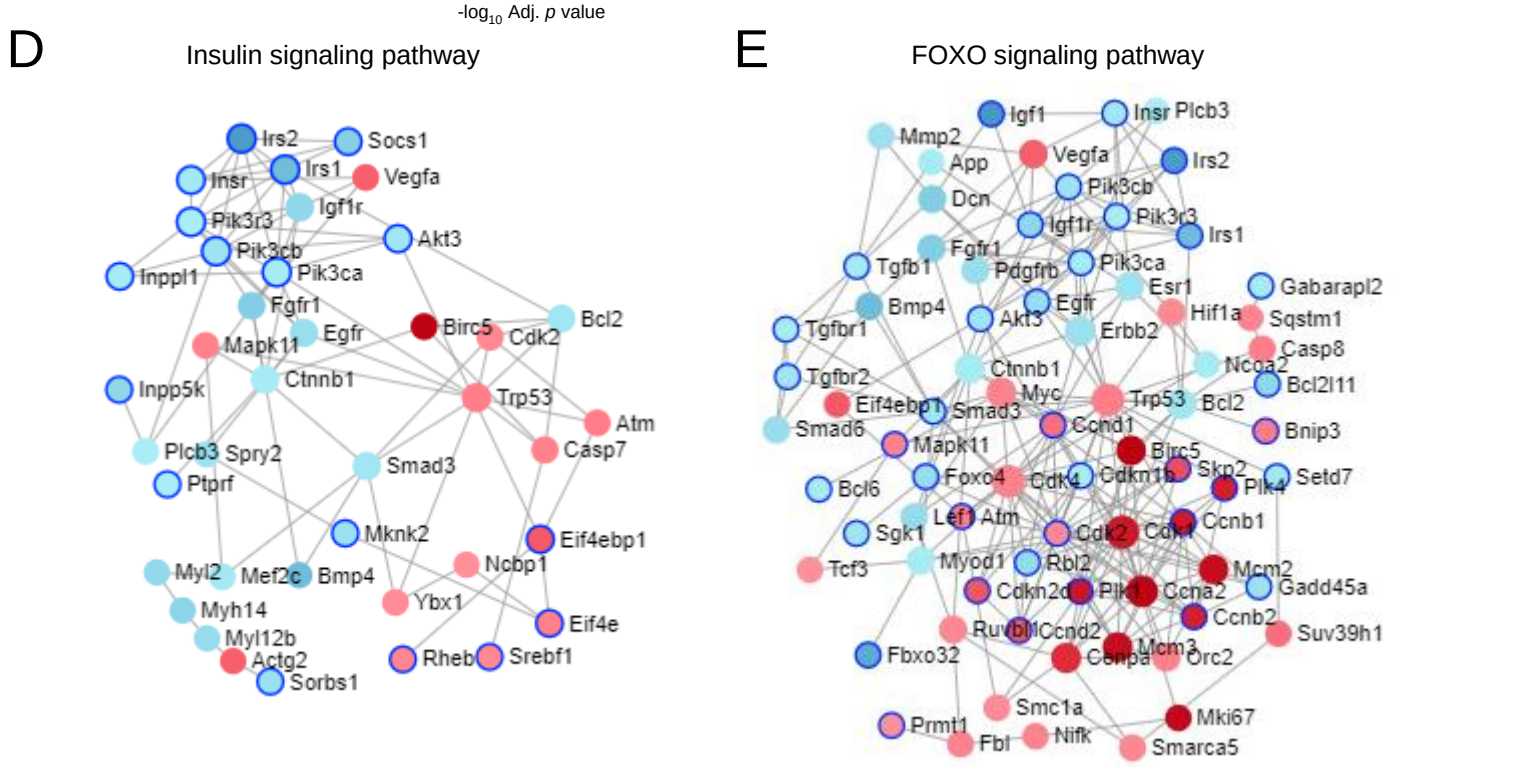

Figure 7. Transcriptomic analysis of hyperinsulinemia and serum starvation.

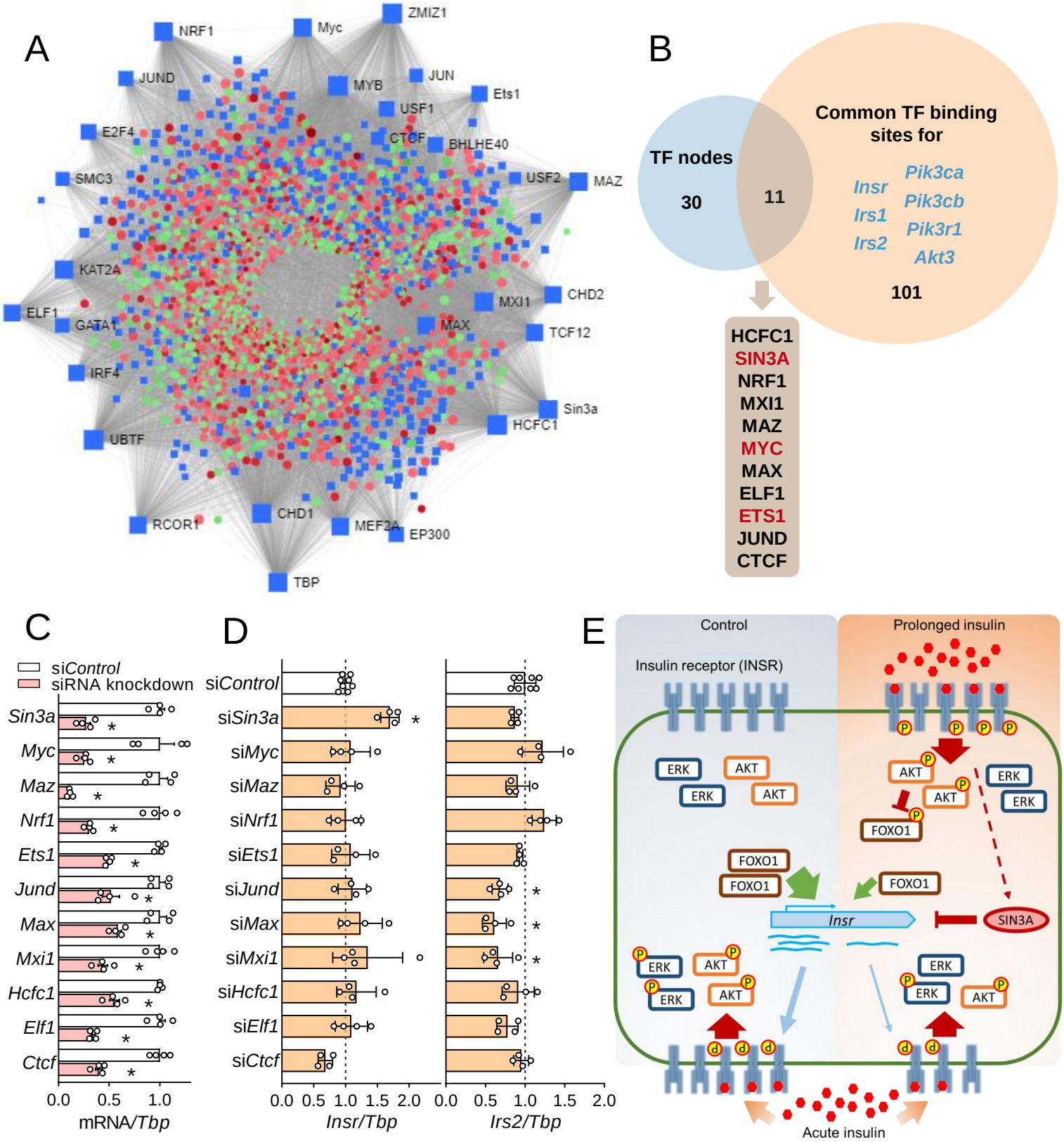

Figure 8. Identification of upstream transcription factors mediating the overall transcriptomic changes and insulin receptor expression.

Supplementary Figures

Figure S1. Transcriptomic analysis of hyperinsulinemia and serum starvation. (A) Top 20 KEGG pathways enriched from up or down regulated genes in all 4 comparisons of insulin and starvation treatments. **(B)** RAS and MAPK signaling, and **(C)** PI3K-AKT signaling pathways enriched in the PPI network of deferentially expressed genes by hyperinsulinemia before starvation (BS, 0 vs 200 nM insulin).

Figure S2. Alterations in KEGG pathways. Differentially expressed genes altered by hyperinsulinemia before starvation (BS, 0 vs 200 nM insulin) are mapped to corresponding proteins in **(A)** Insulin signaling, **(B)** PI3K-AKT signaling, **(C)** RAS and **(D)** MAPK, and **(E)** FOXO signaling pathways.

A

BS 200 nM vs BS 0 nM	Hits/Total	AS 200 nM vs AS 0 nM	Hits/Total	AS 200 nM vs BS 200 nM	Hits/Total	AS 0 nM vs BS 0 nM	Hits/Total
Ribosome	103/175	Ribosome	75/175	Autophagy - animal	29/130	HIF-1 signaling pathway	17/105
Spliceosome	77/133	DNA replication	32/35	Herpes simplex infection	64/439	Glycolysis / Gluconeogenesis	11/67
Cell cycle	68/123	Cell cycle	55/123	Pathways regulating pluripotency of stem cells	29/137	Central carbon metabolism in cancer	8/64
RNA transport	80/167	Homologous recombination	22/41	FoxO signaling pathway	27/132	Pathways in cancer	20/535
DNA replication	32/35	Mismatch repair	16/22	Circadian rhythm	10/30	Carbon metabolism	9/120
Homologous recombination	27/41	Fanconi anemia pathway	23/51	Pathways in cancer	66/535	Galactose metabolism	5/32
Mismatch repair	19/22	Nucleotide excision repair	21/43	Notch signaling pathway	12/49	Biosynthesis of amino acids	7/78
Fanconi anemia pathway	27/51	Base excision repair	16/35	Hepatitis B	26/163	Fructose and mannose metabolism	5/35
Base excision repair	21/35	Oocyte meiosis	28/116	Inositol phosphate metabolism	15/73	Thyroid hormone signaling pathway	8/115
Ribosome biogenesis in eukaryotes	41/116	p53 signaling pathway	21/71	PI3K-Akt signaling pathway	46/358	AGE-RAGE pathway in diabetic complications	7/101
Nucleotide excision repair	21/43	RNA transport	34/167	Prostate cancer	18/97	Metabolic pathways	35/1490
RNA degradation	31/83	Progesterone-mediated oocyte maturation	21/90	Longevity regulating pathway	17/90	Amino sugar and nucleotide sugar metabolism	5/49
Biosynthesis of amino acids	29/78	Spliceosome	26/133	Kaposi's sarcoma-associated herpesvirus infection	31/217	Pentose phosphate pathway	4/32
Progesterone-mediated oocyte maturation	30/90	Pyrimidine metabolism	14/58	Peroxisome	16/84	Protein processing in endoplasmic reticulum	8/163
mRNA surveillance pathway	31/96	RNA degradation	16/83	AMPK signaling pathway	21/126	Renal cell carcinoma	5/68
Protein processing in endoplasmic reticulum	44/163	Carbon metabolism	19/120	TGF-beta signaling pathway	17/93	Glucagon signaling pathway	6/102
Oocyte meiosis	34/116	Glycolysis / Gluconeogenesis	13/67	Acute myeloid leukemia	14/69	Thyroid hormone synthesis	5/73
Aminoacyl-tRNA biosynthesis	23/66	mRNA surveillance pathway	16/96	Chagas disease (American trypanosomiasis)	18/103	Insulin secretion	5/86
Cellular senescence	47/186	Non-homologous end-joining	5/13	Mitophagy - animal	13/63	Autophagy - animal	6/130
Carbon metabolism	34/120	One carbon pool by folate	6/19	Thyroid hormone signaling pathway	19/115	Starch and sucrose metabolism	3/33
Pathways in cancer	98/535	Dilated cardiomyopathy	23/90	Spliceosome	40/133	Ribosome biogenesis in eukaryotes	14/116
EGFR tyrosine kinase inhibitor resistance	26/80	Hypertrophic cardiomyopathy (HCM)	22/86	DNA replication	18/35	Glutathione metabolism	6/64
Autophagy - animal	35/130	Arrhythmogenic right ventricular cardiomyopathy	18/72	Biosynthesis of amino acids	27/78	Ferroptosis	5/41
FoxO signaling pathway	35/132	Rap1 signaling pathway	32/209	RNA transport	42/167	Drug metabolism - cytochrome P450	6/68
Arrhythmogenic right ventricular cardiomyopathy	24/72	MAPK signaling pathway	32/294	HIF-1 signaling pathway	31/105	Tyrosine metabolism	4/40
Dilated cardiomyopathy	27/90	Focal adhesion	32/199	Metabolic pathways	194/1490	Spliceosome	7/133
Hypertrophic cardiomyopathy (HCM)	26/86	Axon guidance	25/180	Carbon metabolism	31/120	RNA transport	7/167
Prostate cancer	27/97	Regulation of actin cytoskeleton	28/217	Purine metabolism	32/136	RNA polymerase	3/30
Ras signaling pathway	48/233	TNF signaling pathway	17/110	Aminoacyl-tRNA biosynthesis	20/66	Circadian rhythm	3/30
Hippo signaling pathway	36/154	Adrenergic signaling in cardiomyocytes	20/148	Ribosome biogenesis in eukaryotes	28/116	beta-Alanine metabolism	3/32
Endocytosis	53/270	cGMP-PKG signaling pathway	22/172	Cell cycle	29/123	Metabolism of xenobiotics by cytochrome P450	4/66
Inositol phosphate metabolism	21/73	Leukocyte transendothelial migration	17/115	Protein processing in endoplasmic reticulum	34/163	Glycolysis / Gluconeogenesis	4/67
Axon guidance	38/180	Prostate cancer	15/97	Small cell lung cancer	23/92	Selenocompound metabolism	2/17
HIF-1 signaling pathway	26/105	EGFR tyrosine kinase inhibitor resistance	13/80	Pyrimidine metabolism	17/58	Carbon metabolism	5/120
Proteoglycans in cancer	41/204	HIF-1 signaling pathway	15/105	Cellular senescence	36/186	Mineral absorption	3/45
AGE-RAGE pathway in diabetic complications	25/101	Jak-STAT signaling pathway	20/165	One carbon pool by folate	9/19	Cysteine and methionine metabolism	3/50
Phosphatidylinositol signaling system	24/98	Proteoglycans in cancer	23/204	Glycolysis / Gluconeogenesis	18/67	Arginine and proline metabolism	3/50
MAPK signaling pathway	52/294	Ras signaling pathway	25/233	Protein export	10/28	Chemical carcinogenesis	4/94
Wnt signaling pathway	33/160	Glioma	12/75	Central carbon metabolism in cancer	16/64	Phenylalanine metabolism	2/23
Regulation of actin cytoskeleton	41/217	Insulin secretion	13/86	p53 signaling pathway	17/71	Histidine metabolism	2/24

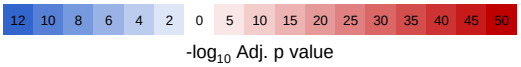

B

RAS & MAPK signaling pathway

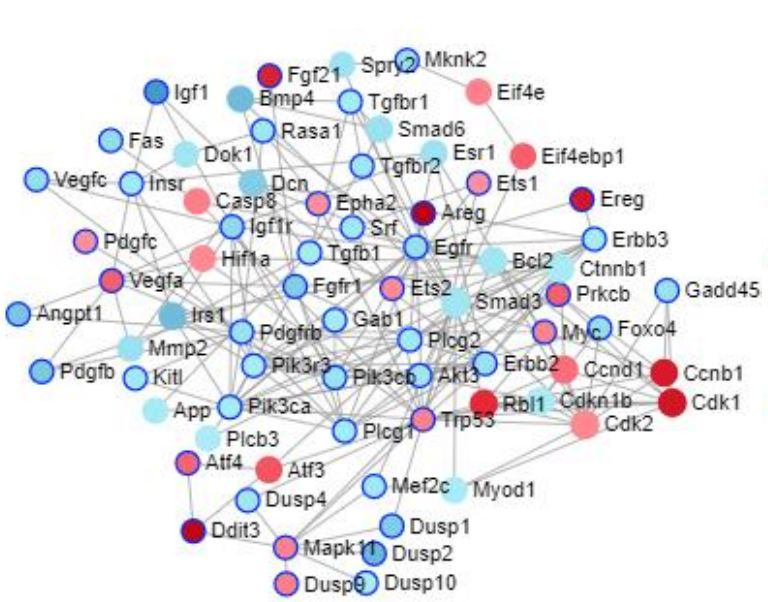

C

PI3K-AKT signaling pathway

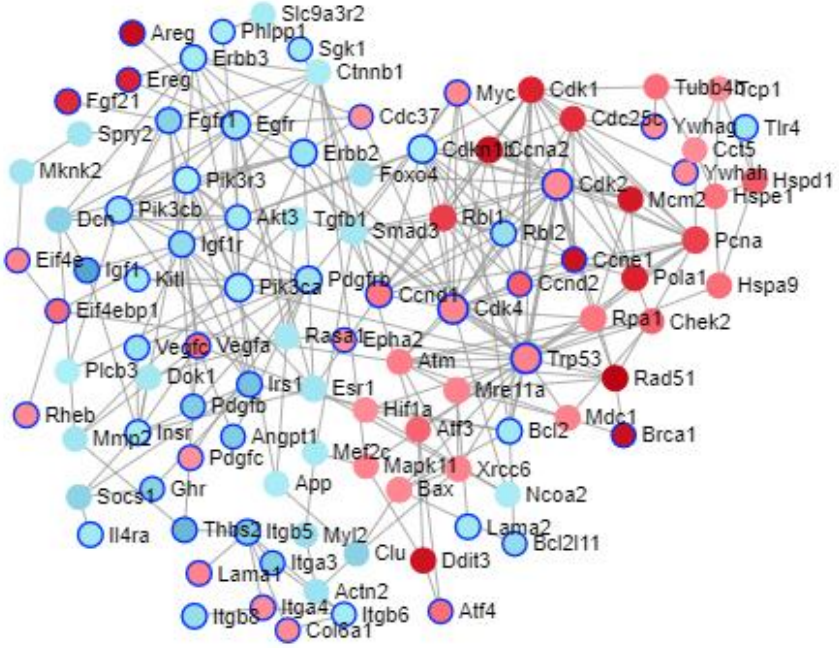

Figure S1. Transcriptomic analysis of hyperinsulinemia and serum starvation.

A

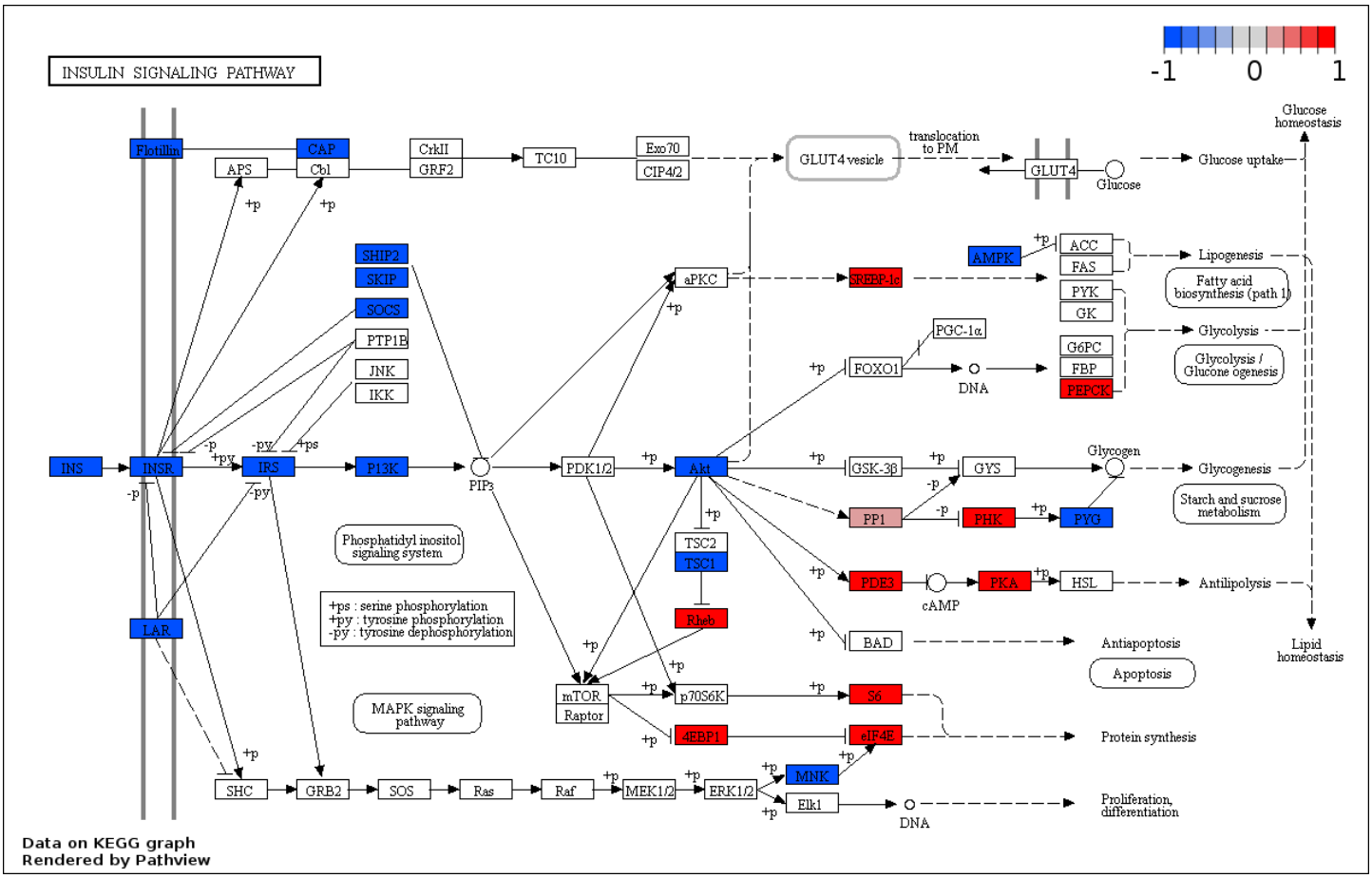

B

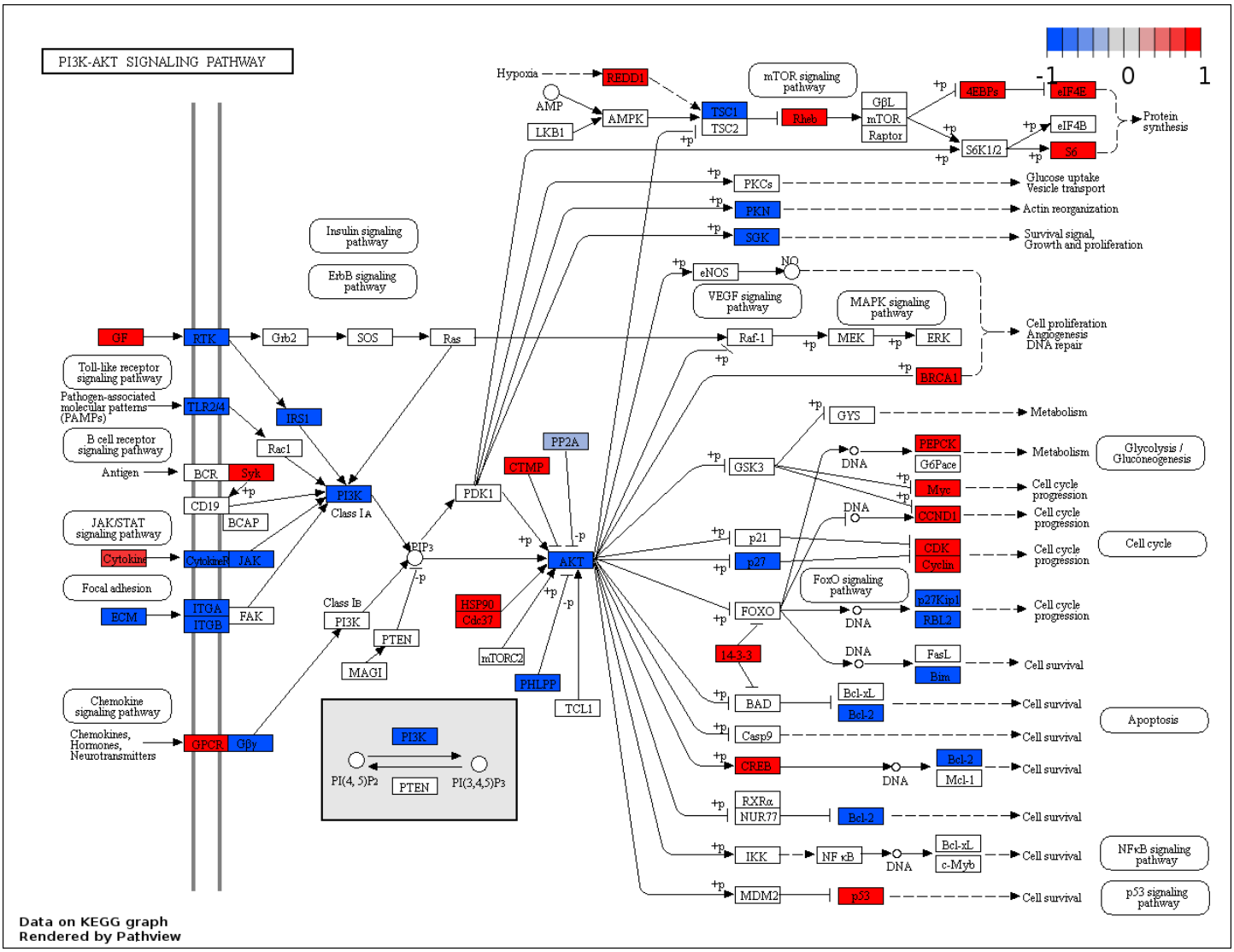

Figure S2. Alterations in KEGG pathways.

C

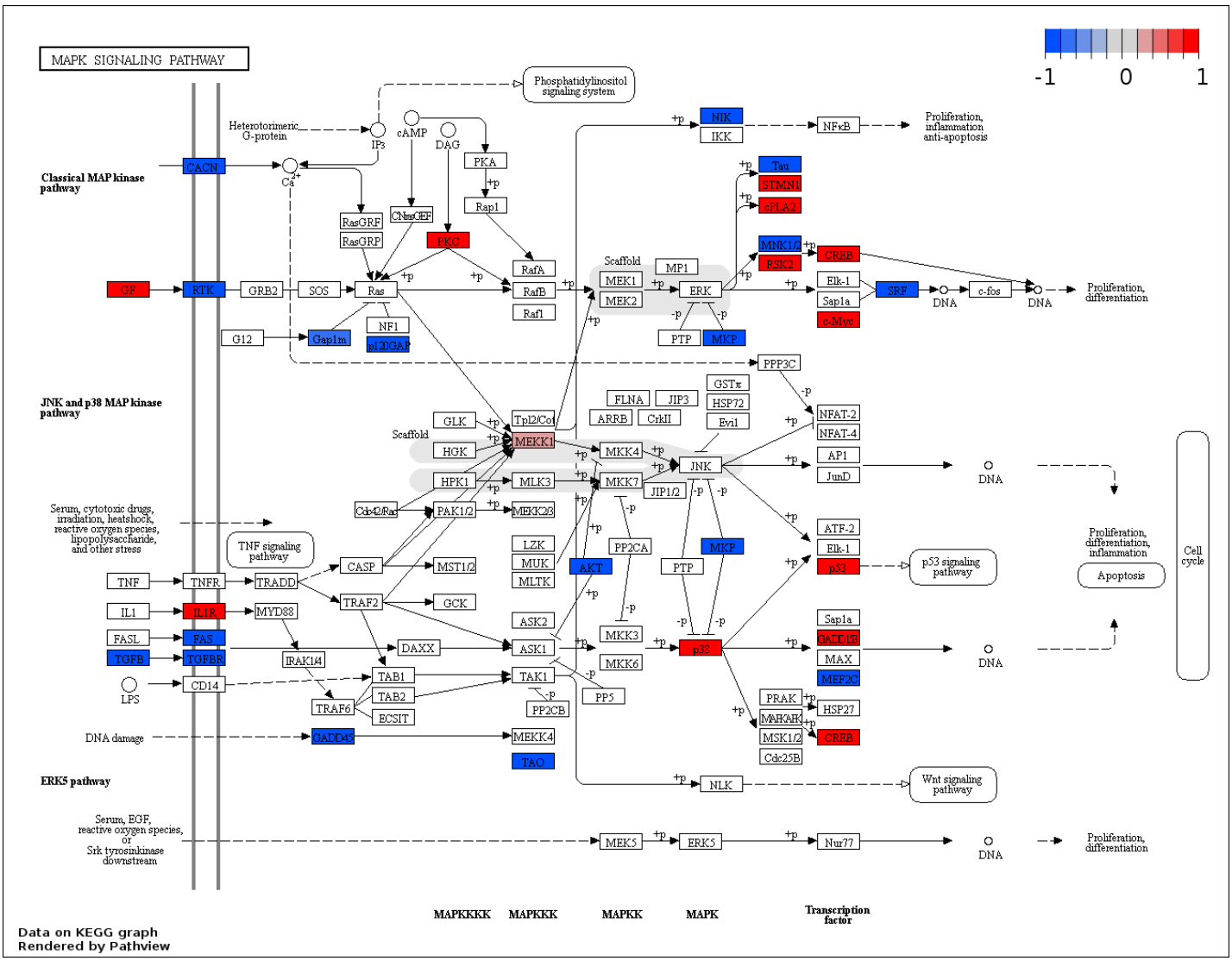

D

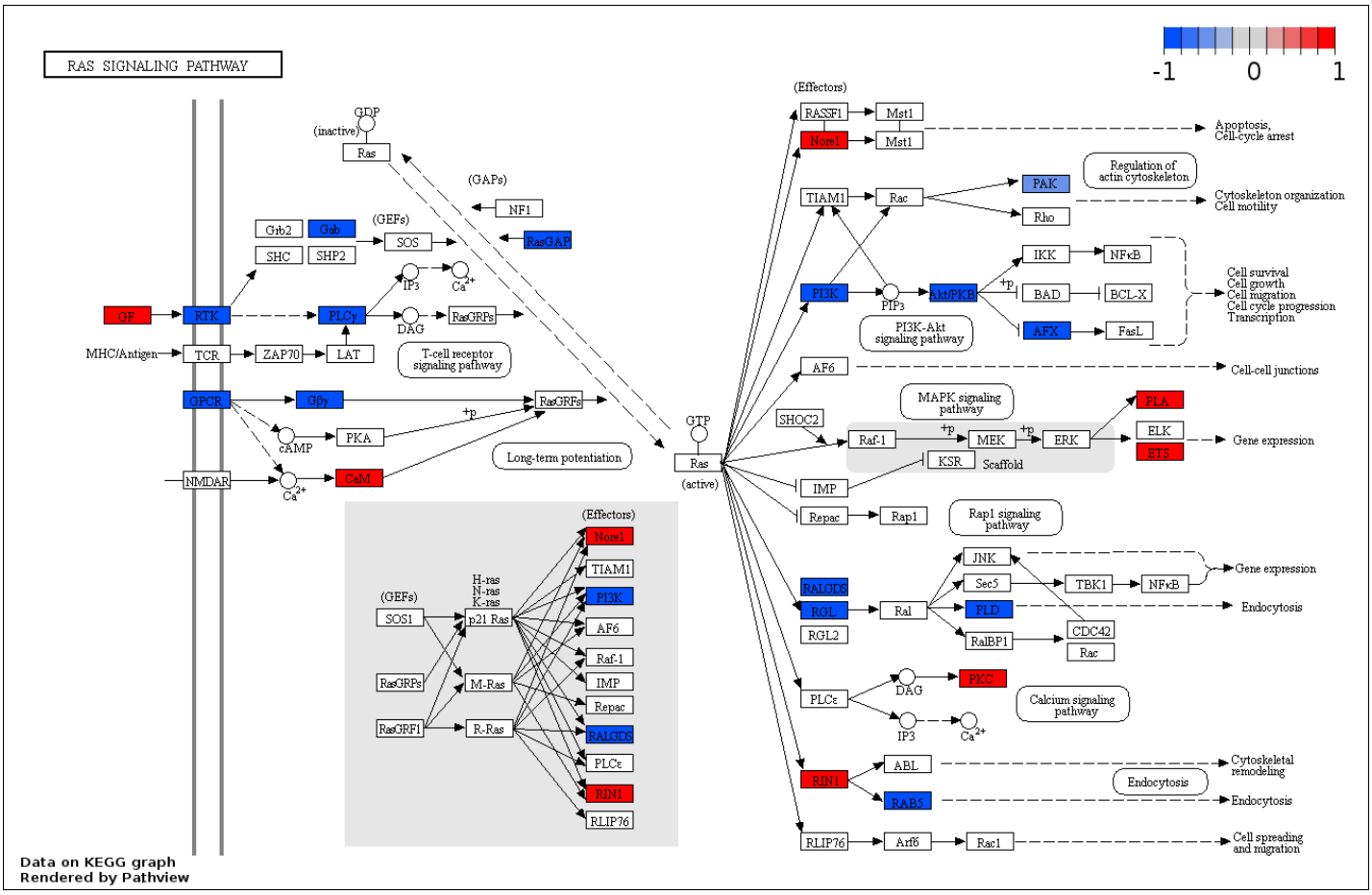

Figure S2. Alterations in KEGG pathways.

E

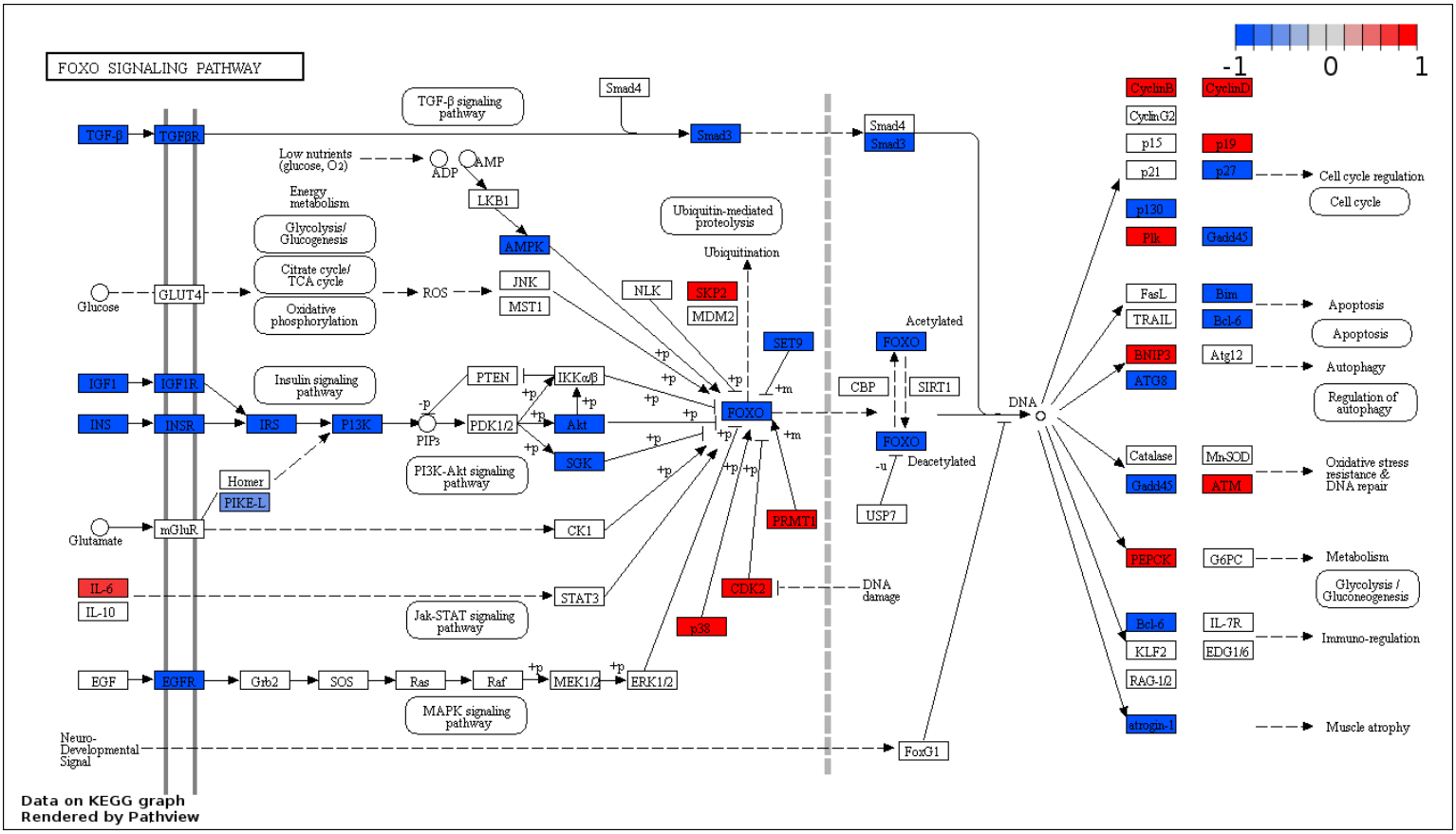

Figure S2. Alterations in KEGG pathways.